



The case and context for atmospheric methane as an exoplanet biosignature

Maggie A. Thompson^{a,1}, Joshua Krissansen-Totton^a, Nicholas Wogan^b, Myriam Telus^c, and Jonathan J. Fortney^a

Edited by Neta Bahcall, Princeton University, Princeton, NJ; received October 8, 2021; accepted January 31, 2022

Methane has been proposed as an exoplanet biosignature. Imminent observations with the James Webb Space Telescope may enable methane detections on potentially habitable exoplanets, so it is essential to assess in what planetary contexts methane is a compelling biosignature. Methane's short photochemical lifetime in terrestrial planet atmospheres implies that abundant methane requires large replenishment fluxes. While methane can be produced by a variety of abiotic mechanisms such as outgassing, serpentinizing reactions, and impacts, we argue that—in contrast to an Earth-like biosphere—known abiotic processes cannot easily generate atmospheres rich in CH₄ and CO₂ with limited CO due to the strong redox disequilibrium between CH₄ and CO₂. Methane is thus more likely to be biogenic for planets with 1) a terrestrial bulk density, high mean-molecular-weight and anoxic atmosphere, and an old host star; 2) an abundance of CH₄ that implies surface fluxes exceeding what could be supplied by abiotic processes; and 3) atmospheric CO₂ with comparatively little CO.

methane | biosignatures | planetary atmospheres

The next phase of exoplanet science will focus on characterizing exoplanet atmospheres, including those of potentially habitable planets. For example, the James Webb Space Telescope (JWST) will be capable of characterizing the atmospheres of transiting, terrestrial planets around low-mass stars, such as the TRAPPIST-1 system (1, 2). A new class of ground-based telescopes (3) may be able to detect atmospheric constituents such as oxygen, water, and carbon dioxide on nearby rocky exoplanets via high-resolution spectroscopy (4). In subsequent decades, the Astro2020 Decadal Survey report has prioritized a large infrared/optical/ultraviolet (UV) telescope built to search for signs of life—biosignatures—on ~25 habitable-zone planets (5). Life may modify its planetary environment in multiple ways, including producing waste gases that alter a planet's atmospheric composition. As a result, an understanding of detectable biogenic waste gases and their nonbiological false positives is needed.

Terrestrial planets, which are the focus of this study, require significant methane surface fluxes to sustain high atmospheric abundances. On Earth, life sustains large methane surface fluxes, and so methane has long been regarded as a potential biosignature gas for terrestrial exoplanets. Previous studies have considered abiotic methane production (6–11), methane biosignatures in the context of chemical disequilibrium (12–15), and prospects for remote detection of methane in terrestrial atmospheres (6, 9, 15–17). During the Archean eon (4 to 2.5 Ga), Earth's atmosphere likely had high methane abundances (~10² to 10⁴ times modern) due to life (i.e., methanogenesis) (8, 18, 19). Methane is thus not a hypothetical biosignature because we know of an inhabited terrestrial planet with detectable levels of biogenic methane—the Archean Earth. However, methane is sometimes dismissed as irredeemably ambiguous due to its ubiquity in planetary environments and potential for nonbiological production (8, 9). Additional work is clearly needed to understand methane biosignatures and their false positives within different planetary contexts.

While other studies have reviewed the biosignature gases oxygen (20), phosphine (21), isoprene (22), and ammonia (23), in the near term, these gases will likely be difficult to detect or will be detectable only in extended H₂-dominated atmospheres on planets with large biogenic fluxes. In contrast, for Earth-like biogenic fluxes, methane is one of the few biosignatures that may be readily detectable with JWST (24–26). For example, biological methane on an early Earth-like TRAPPIST-1e could be detectable with 5 to 10 transits with JWST (17, 27) and would remain detectable even with an optically thick aerosol layer at 10 to 100 mbar, assuming plausible instrument noise and negligible stellar contamination (17).

Given the imminent feasibility of observing methane with JWST, it is imperative to determine the planetary conditions where methane is a compelling biosignature. Despite the patchwork of past studies on methane biosignatures, a recent and dedicated investigation

Significance

Astronomers will soon begin searching for biosignatures, atmospheric gases or surface features produced by life, on potentially habitable planets. Since methane is the only biosignature that the James Webb Space Telescope could readily detect in terrestrial atmospheres, it is imperative to understand methane biosignatures to contextualize these upcoming observations. We explore the necessary planetary context for methane to be a persuasive biosignature and assess whether, and in what planetary environments, abiotic sources of methane could result in false-positive scenarios. With these results, we provide a tentative framework for assessing methane biosignatures. If life is abundant in the universe, then with the correct planetary context, atmospheric methane may be the first detectable indication of life beyond Earth.

Author affiliations: ^aDepartment of Astronomy and Astrophysics, University of California, Santa Cruz, CA 95064; ^bDepartment of Earth and Space Sciences, University of Washington, Seattle, WA 98195; and ^cDepartment of Earth and Planetary Sciences, University of California, Santa Cruz, CA 95064

Author contributions: J.K.-T. designed research; M.A.T., J.K.-T., and N.W. performed research; M.A.T., J.K.-T., and N.W. analyzed data; and M.A.T., J.K.-T., N.W., M.T., and J.J.F. wrote the paper.

The authors declare no competing interest.

This article is a PNAS Direct Submission.

Copyright © 2022 the Author(s). Published by PNAS. This open access article is distributed under Creative Commons Attribution License 4.0 (CC BY).

¹To whom correspondence may be addressed. Email: maaphom@ucsc.edu.

This article contains supporting information online at <https://www.pnas.org/lookup/suppl/doi:10.1073/pnas.2117933119/-DCSupplemental>.

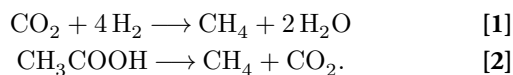
Published March 30, 2022.

into the conditions needed for atmospheric methane to be a good exoplanet biosignature is lacking. This study provides an updated assessment of the necessary planetary context for methane biosignatures. First, we present the case for methane as a biosignature, including its short photochemical lifetime and relationship with chemical disequilibrium and CO antibiosignatures. We then explore the possibility of abiotic methane fluxes as large as those caused by known biogenic sources, in part using different modeling tools. We also discuss the purported presence of methane on Mars and simulate atmospheric methane on temperate Titan-like exoplanets. Based on these results, we propose a framework for identifying methane biosignatures and discuss detectability prospects with next-generation missions.

Biological Methane Production on Earth

The vast majority of methane in Earth's atmosphere today, and throughout most of its history, is biogenic. At present, Earth's ~ 30 Tmol/y global methane emissions are predominantly produced directly by life (including anthropogenic sources), and most of the rest is thermogenic methane that derives from previous life, such as metamorphic reactions of organic matter (28). Genuinely abiotic methane emissions, while uncertain, are comparatively tiny (28).

Biological methane production, or methanogenesis, is a simple metabolism performed by anaerobic microbes (i.e., those not requiring oxygen for growth). Methanogenic microbes can be divided into three groups: hydrogenotrophic (reaction 1), acetoclastic (reaction 2), and methylotrophic methanogens:



Hydrogenotrophic methanogens typically oxidize H_2 and reduce CO_2 to CH_4 and contribute approximately one-third of current biogenic methane emissions. Acetoclastic methanogens use acetate, contributing approximately two-thirds of current biogenic methane emissions; and finally, methylotrophic methanogens use methylated compounds but do not contribute significantly to global biogenic methane emissions (29). Methane can also be produced indirectly by life as a byproduct of degrading organic matter from dead organisms, called "thermogenic methane."

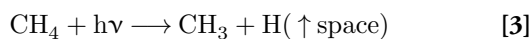
If life elsewhere is common, methanogenesis may be widespread due to the likely ubiquity of the $\text{CO}_2 + \text{H}_2$ redox couple in terrestrial planet atmospheres and the potential metabolic payoff from exploiting such commonly outgassed substrates. Methanogenesis is an ancient metabolism on Earth with phylogenetic analyses implying that methanogenesis originated between 4.11 and 3.78 Ga and reconstructions of the last universal common ancestor suggesting methanogens were one of the earliest lifeforms to evolve on Earth (30–32).

There are several reasons to expect methane-cycling biospheres to produce large CH_4 fluxes. During the Archean, xenon isotopes—which ostensibly reflect abundances of escaping, hydrogen-bearing species in the upper atmosphere—likely imply large methane abundances ($>0.5\%$) (19, 33). This Xe isotope fractionation can potentially be explained by another hydrogen-bearing species (e.g., $>1\%$ H_2 or $>1\%$ H_2O), but such explanations are tentatively disfavored: Catling and Zahnle (19) and Kadoya and Catling (34) place an upper limit of H_2 in the Archean atmosphere of 1% and other paleo-pressure and surface temperature estimates likely preclude $>1\%$ H_2O above the tropopause. Moreover, multiple ecosystem models for the Archean Earth estimate large biogenic CH_4 fluxes and

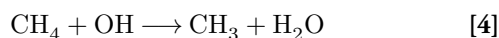
abundant atmospheric CH_4 (35–38). Motivated by observations of inefficient methane generation in a ferruginous, sulfate-poor lake ostensibly representative of Precambrian conditions, biogeochemical models of low Precambrian methane have been proposed (39). However, ref. 40 found that such model behavior is dictated by arbitrary forcings and is not compatible with the rock record. In any case, hydrogenotrophic methanogenesis in the Archean water column could maintain substantial CH_4 fluxes regardless of organic burial efficiency in sediments (35, 38, 39).

Results

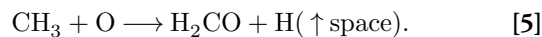
The Case for Methane as a Biosignature. Methane has been highlighted as a potential biosignature gas because it has a short photochemical lifetime (less than ~ 1 My) on habitable-zone, rocky planets orbiting solar-type stars. A short photochemical lifetime requires substantial replenishment fluxes to sustain large atmospheric abundances. Methane is removed from an atmosphere photochemically in two ways, depending on the concentration of CO_2 relative to CH_4 and the presence of other oxidants (41). In the case where CO_2 is significantly more abundant, CH_4 is destroyed by oxidants and is converted to CO_2 (see *SI Appendix, section 3* for additional reactions):



or



and, subsequently,



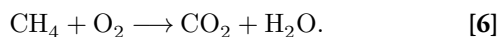
The C in H_2CO is further oxidized to CO_2 . The H produced can then be lost to space, thereby irreversibly destroying CH_4 . Note that OH and O are byproducts of H_2O and CO_2 photolysis; an O_2 -rich atmosphere is not required for rapid CH_4 destruction, although it does decrease the CH_4 lifetime.

For the case where CH_4 is more abundant than CO_2 , CH_4 polymerizes to aerosols, which fall to the ground and remove the atmospheric CH_4 (see *SI Appendix, section 3* for sequence of reactions). If temperatures are high enough in the lower atmosphere, these aerosols could break down and release CH_4 back into the atmosphere. In addition, surface deposition and subsequent thermal decomposition in the subsurface could release methane back into the atmosphere. However, some portion of the hydrogen produced by methane photolysis is lost to space, and so, without H_2 replenishment, the C:H ratio of condensate material will rise such that the methane is irreversibly lost.

The short atmospheric lifetime of terrestrial planet methane can be quantified. Using the photochemical model PhotochemPy adapted from the Atmos code (42) and created by N. Wogan (43) (*SI Appendix, section 6A*), we explore the stability of atmospheric CH_4 for an Archean Earth-like planet (i.e., N_2 - CO_2 - CH_4) orbiting a 2.7-Ga Sun-like star. Every calculation conserves redox. Consistent with previous studies (7, 13, 44, 45), we find that for atmospheric CH_4 mixing ratios greater than $\sim 10^{-3}$ to be stable against photochemistry requires replenishing CH_4 surface fluxes that are larger than Earth's current biological flux (*SI Appendix, Fig. S1*). If a planet is orbiting a different stellar-type host star, it will be necessary to recalculate the threshold for biological methane surface fluxes. For example, planets orbiting M-stars tend to have lower near-UV radiation compared to Sun-like stars, which reduces the OH produced by H_2O photolysis, permitting higher atmospheric CH_4 concentrations (46). Ultimately, however, a terrestrial planet atmosphere that is rich in CH_4

cannot persist unless there is a significant replenishment source flux, making it an intriguing candidate for further investigation.

Methane biosignatures and chemical disequilibrium. The methane biosignature case is strengthened if its presence in the atmosphere is accompanied by that of a strongly oxidizing companion gas such as CO₂ or O₂/O₃. This is because it is difficult to explain abundant methane if a terrestrial planet's atmospheric redox state is sufficiently oxidized such that the thermodynamically stable form of carbon is not CH₄. Methane in O₂-rich atmospheres requires large replenishment fluxes because CH₄ and O₂ are kinetically unstable and out of thermodynamic equilibrium (47, 48). The kinetic lifetime of methane in O₂-rich atmospheres is ~10 y (44) due to the following net reaction, which is the end result of reactions 3 to 5 above after the H₂CO has been further oxidized to CO₂:



Another important thermodynamic disequilibrium is that between CH₄ and CO₂, which was present on the Archean Earth prior to the rise of O₂. Specifically, CH₄, CO₂, N₂, and liquid H₂O coexisted out of equilibrium on the early Earth due to the replenishment of CH₄ by life (14). In a weakly reduced Archean atmosphere, CH₄'s lifetime would have been short (up to ~2,000 to 20,000 y) compared to geologic timescales (49, 50). This short kinetic lifetime of methane does not depend on this thermodynamic disequilibrium with CO₂; methane has a short photochemical lifetime in high mean-molecular-weight atmospheres regardless of whether or not CO₂ is present in abundance. However, the thermodynamic disequilibrium is of fundamental importance for the discussion of abiotic methane that follows. Crucially, CH₄ and CO₂ are at opposite ends of the redox spectrum for carbon, separated by eight electrons. This has implications for how both species can be produced via abiotic planetary interior processes, which we explore subsequently; see the discussion of CO below. On the basis of both this thermodynamic disequilibrium and methane's short photochemical lifetime, Krissansen-Totton et al. (14) argued that detecting both abundant CH₄ and CO₂ in a habitable-zone rocky exoplanet may be a biosignature and, if CH₄'s mixing ratio is greater than ~0.001, the methane is probably biogenic because it is challenging for abiotic sources to sustain large methane fluxes in anoxic atmospheres, similar to the findings of ref. 6.

CO antibioticsignatures and their relationship to CH₄ biosignatures.

In the above scenario, the absence of significant atmospheric CO may strengthen the case for biogenic CH₄ since 1) microbial life readily consumes CO, a source of free energy, and 2) many abiotic processes that produce CH₄ also result in abundant CO (14, 51) (and see below on magmatic outgassing). Life on Earth metabolizes CO because oxidizing it with water yields free energy and because CO metabolism serves as a starting point for carbon fixation (52, 53). Multiple lines of evidence suggest that CO consumption could be a ubiquitous metabolic strategy given its ancient origin on Earth (32, 53–55) and because the required enzymes possess a variety of simple Ni-Fe, Mo, or Cu active sites, suggesting that they have evolved independently multiple times (53, 56, 57). However, the mere presence or absence of CO may not be an unambiguous discriminator between a CH₄-producing biosphere and an uninhabited world. An inhabited planet may have CH₄, CO₂, and some CO in its atmosphere if life is unable to efficiently consume all of the CO (11, 37, 38). In this case, however, the CO/CH₄ atmospheric ratio in terrestrial planets' high mean-molecular-weight atmospheres could potentially be used as a diagnostic tool to distinguish anoxic, inhabited planets from

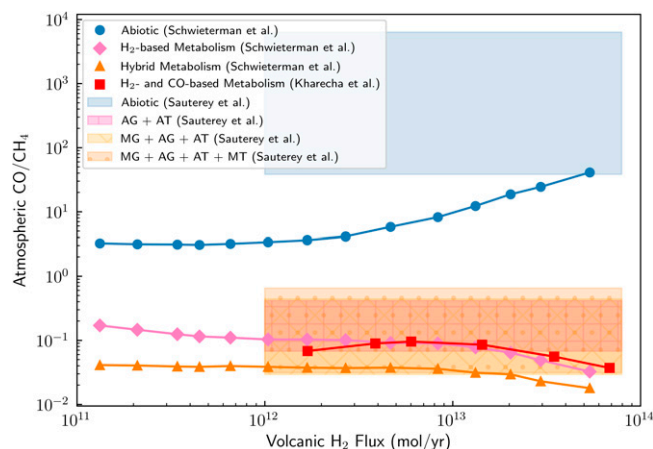


Fig. 1. Atmospheric CO to CH₄ ratio may help distinguish biogenic and abiotic methane. Shown is ratio of atmospheric CO to CH₄ for abiotic worlds and those with biospheres as a function of volcanic H₂ flux. The curves show the calculated atmospheric CO/CH₄ as a function of volcanic H₂ flux for abiotic worlds (blue circles), H₂-based biospheres (includes H₂-consuming anoxygenic photosynthesis, CO-consuming acetogenesis, organic matter fermentation, and acetotrophic methanogenesis) (pink diamonds), H₂-based and Fe-based photosynthesis biospheres (i.e., “hybrid,” orange triangles) from ref. 37, and the methanogen–acetogen ecosystem and anoxygenic phototroph–acetogen ecosystem from ref. 35 (i.e., their cases 2 and 3) (red squares). The horizontal shaded regions correspond to the distributions of atmospheric CO/CH₄ for abiotic worlds (blue) and those with methanogenic biospheres (pink, yellow, and orange) as a function of volcanic H₂ flux calculated by ref. 38. The atmospheric CO/CH₄ for abiotic worlds is predicted to be several orders of magnitude greater than that for inhabited worlds. Refs. 35, 37, and 38 found that low CO/CH₄ atmospheric ratios (~0.1) are a strong sign of methane-cycling biospheres for reducing planets orbiting Sun-like stars like Archean Earth, suggesting that atmospheric CO/CH₄ is a good observable diagnostic tool to distinguish abiotic planets from those with anoxic biospheres. The light pink “+”-hatched region corresponds to an ecosystem with CO-based autotrophic acetogens (AG) and methanogenic acetotrophs (AT); the light orange “X”-hatched region corresponds to an ecosystem with H₂-based methanogens (MG), AG, and AT; the orange “-”-hatched region corresponds to the most complex ecosystem consisting of MG, AG, AT, and anaerobic methanotrophy (MT) (38). All calculations assume a CO₂-CH₄-N₂ bulk atmosphere.

lifeless worlds because the CO/CH₄ atmospheric ratio reflects the fractional atmospheric free energy that has been exploited.

Kharecha et al. (35), Schwieterman et al. (37), and Sauterey et al. (38) found that the atmospheric CO/CH₄ ratio for abiotic worlds is predicted to be approximately two orders of magnitude larger than that for inhabited worlds that have anoxic biospheres over a wide range of volcanic H₂ fluxes (Fig. 1). Note that we consider only the ecosystems from refs. 35 and 38 where both methanogenesis and CO consumption (acetogenesis plus acetotrophy) have evolved; if these conditions are not met, then larger CO/CH₄ ratios are possible, but note the arguments for rapid emergence of CO consumption outlined above. While the atmospheric CO/CH₄ ratio is likely an observable parameter that can be used to distinguish lifeless from inhabited, anoxic worlds, additional modeling is required to explore the possible range of CH₄, CO₂, and CO abundances for a wide variety of biospheres and uninhabited worlds around different host star types.

Abiotic Sources of Methane. While the vast majority of Earth's atmospheric methane is produced biotically (28), there are various small abiotic sources of methane that could potentially be enhanced on other planets. Understanding plausible abiotic methane fluxes is necessary for discriminating methane biosignature false-positive scenarios from true signs of metabolism. These abiotic sources can be broadly divided into the following categories (Fig. 2): 1) volcanism and high-temperature magmatic processes,



Fig. 2. Summary of known abiotic sources of methane on Earth (© 2022 Elena Hartley) (<http://www.elabarts.com>). In general, the abiotic sources of methane can be divided into three categories: high-temperature magmatic outgassing (volcanism), low-temperature water-rock and metamorphic reactions, and impacts. Currently, subaerial (submarine) volcanoes on Earth generate only $\leq 10^{-3}$ ($\sim 10^{-2}$) Tmol/y of methane (see main text). Low-temperature water-rock reactions that generate methane occur at midocean ridges, deep-sea hydrothermal vents, subduction zones, and continental settings. Methane can also be generated by metamorphic reactions, particularly in subduction zones and continental settings such as ophiolites, orogenic massifs, and Precambrian shields. Both water-rock and metamorphic reactions can generate variable quantities of methane depending on the geochemical conditions, but, on Earth, methane fluxes are orders of magnitude smaller than biological sources. Finally, impacts or other exogenous sources can generate methane. The impact flux was larger during earlier periods in Earth's history, and such large impact fluxes are necessary to generate significant methane. A critical factor that influences the amount of methane that can be generated via all of these processes is the source of reducing power; in comparatively oxidizing surface environments with abundant CO_2 , a reductant is needed to reduce carbon to CH_4 . For magmatic outgassing, the reducing power ultimately comes from the mantle, with more reduced mantles outgassing more methane relative to CO_2 and CO . For low-temperature water-rock and metamorphic reactions, the key source of reducing power is ferrous iron (Fe^{2+}) in the crust, and in some cases the redox state of the mantle can also influence methane generation. For impact events, the metallic or ferrous iron that is delivered by the impactor serves as the source of reducing power.

2) low-temperature water-rock and metamorphic reactions, and
3) impact events.

Volcanism/high-temperature magmatic outgassing. Volcanoes on Earth today do not outgas significant methane. Most subaerial volcanoes produce less than $\sim 10^{-6}$ Tmol CH_4 per year (10, 58), and given the $\sim 1,500$ active volcanoes on Earth today, the estimated global CH_4 flux is $< 10^{-3}$ Tmol/y, much less than the current biogenic flux of 30 Tmol/y. Similarly, Schindler and Kasting (6) estimated the CH_4 flux from submarine volcanism to be $\sim 10^{-2}$ Tmol/y. Although mud volcanoes, geological structures that transport clay rocks and sediment from Earth's interior to the surface, can emit large amounts of methane and CO_2 (59), the methane is largely thermogenic, ultimately deriving from organic matter produced by life (60). In principle, a terrestrial planet could abiotically emit methane through mud volcanoes given an abiotic source for the organic matter, such as hydrocarbon deposition from an organic haze. But that organic matter would need to be continuously replenished, and it is challenging for abiotic

sources to provide the necessary replenishment (16, 42), especially under conditions sufficiently oxidizing to maintain a CO_2 -rich atmosphere.

Wogan et al. (11) investigated whether magmatic outgassing could produce genuinely abiotic CH_4 fluxes on terrestrial planets with diverse compositions and surface conditions. They determined that volcanoes are unlikely to produce CH_4 fluxes comparable to Earth's biological flux because water has a high solubility in magma, which limits how much hydrogen (and therefore CH_4) can outgas. Also, CH_4 formation is thermodynamically favorable at temperatures lower than typical magma temperatures on Earth and at magma oxygen fugacities much more reduced than those expected for most terrestrial planets (11).

Could planets with significantly more reduced mantles and crusts produce high CH_4 fluxes via magmatic outgassing? Mercury's silicate interior has a low oxygen fugacity of $\sim 5 \log_{10}$ units below the iron-wüstite (IW) redox buffer, and its crust is enriched in graphite, a crystalline form of carbon (61, 62). While Mercury's

small size and proximity to the Sun preclude the retention of an atmosphere, if there are large terrestrial exoplanets with similarly reducing interiors, then it is important to determine whether magmatic outgassing could produce CH₄-rich atmospheres.

Following the melting and volatile partitioning methods used in ref. 63, we applied a batch melting model, which assumes a partial melt is in equilibrium with the source rock before it rises to the surface, to determine the partitioning of volatiles from the rock to the melt (SI Appendix, section 6B). We assume the partitioning of carbon between the melt and solid phases is controlled by oxygen fugacity-dependent graphite saturation. For the top ~10 km of crust (pressures from ~0 to 0.5 GPa and solidus temperatures from ~1,400 to 1,445 K), we ran a Monte Carlo simulation to explore a range of source rock CO₂ and H₂O concentrations, melt fractions, and planetary melt production volumes with oxygen fugacities from IW–11 to IW+5 (SI Appendix, Table S1). We find that for very reduced melts at or below IW–2, essentially all of the carbon (>99%) will precipitate as graphite during partial melting, so there is negligible carbon available for gaseous phases (Fig. 3 and SI Appendix, Fig. S2), consistent with observations of Mercury's graphite-enriched crust (64). Rocky exoplanets with ultrareduced magma compositions are unlikely to outgas significant quantities of CH₄ due to graphite saturation, although more experiments are needed to confirm reduced magmas' outgassing compositions.

In the rare cases where volcanoes could produce biogenic levels of CH₄ assuming magma production rates larger (>10 times) than those on Earth today, they would also outgas significant amounts of carbon monoxide (CO) gas (11). As described above, the atmospheric CO/CH₄ ratio could be used to distinguish between abiotic (outgassed) and biotic scenarios (11, 37). Ultimately, high-temperature magmatic outgassing, such as through volcanism, is unlikely to produce atmospheric CH₄ fluxes similar to those produced by biology on Earth.

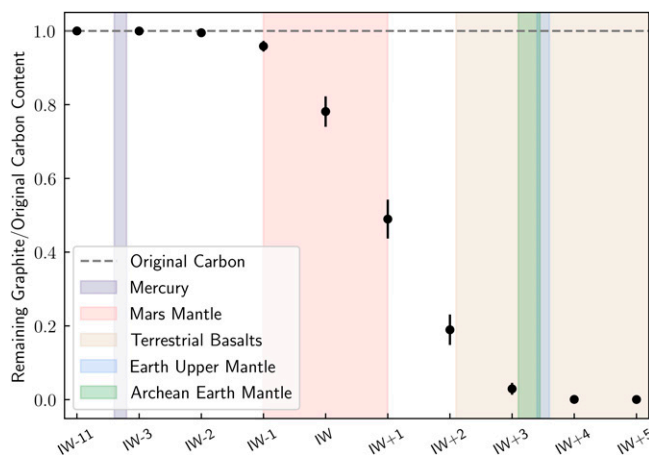
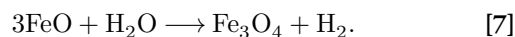
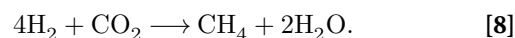


Fig. 3. Most carbon partitions into graphite under reducing conditions and so cannot degas as CH₄. Shown is the ratio of the amount of remaining graphite to the original carbon content as a function of oxygen fugacity. We used a batch-melting model to determine how volatiles would partition between the rock and melt over an ~10-km deep column of newly produced crust with pressures from ~0 to 0.5 GPa and temperatures from 1,400 to 1,445 K (SI Appendix, section 6B). For each oxygen fugacity, we ran a Monte Carlo simulation varying the input parameters, including CO₂ and H₂O mass fractions in the mantle source rock, the fraction of source material that is melted during emplacement, and the planetary melt production rate. The average ratio of remaining graphite to initial carbon content from the Monte Carlo simulation is shown with the uncertainty reported as the 95% confidence interval. The horizontal dashed line (y = 1) illustrates the original amount of carbon, and ratios that fall on this line have all of the original carbon stable as graphite. The shaded vertical regions show the estimated oxygen fugacities of Mercury's lavas (61), the Martian mantle (65), terrestrial basalts (66), Earth's upper mantle (67), and Archean Earth's mantle (68) for reference.

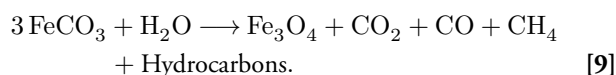
Low-temperature water-rock reactions and metamorphic reactions. The reliability of methane as a biosignature on habitable planets depends upon the tendency of low-temperature (below solidus) systems to generate methane via abiotic reactions. Under oxidizing planetary conditions conducive to CO₂ degassing, low-temperature CH₄ production is ultimately limited by the supply of reducing power in the form of ferrous iron (Fe²⁺) in newly produced crust. One of the most frequently discussed processes for methane production is serpentinization, through which iron-bearing minerals are altered by hydration to produce H₂ via the oxidation of Fe²⁺ by water (10, 69, 70):



Subsequently, H₂ can react with oxidized forms of carbon to produce CH₄ by Fischer–Tropsch-type (FTT) reactions:



Metamorphic reactions may also produce CH₄ via iron oxidation. For example, Fe-bearing carbonates can decompose when metamorphosed and react with water to form CH₄ (71):



Experimental methane and hydrocarbon yields via such reactions are typically very low compared to that of CO₂ (72).

Experimental, observational, and theoretical approaches have been taken to determine the efficiency of hydrothermal and metamorphic processes and their corresponding abiotic CH₄ production fluxes on Earth and how they may apply in other planetary environments. Various geological settings are potentially conducive to CH₄ generation, including midocean ridges, subduction zones, and continental settings. For example, Keir (73) and Cannat et al. (74) investigated the concentrations of CH₄ produced by serpentinization at midocean ridges and both found global abiotic CH₄ fluxes to be about three orders of magnitude smaller than the global biogenic CH₄ flux. Combining observational and theoretical approaches, Catling and Kasting (75) estimated abiotic hydrothermal CH₄ fluxes from both axial and off-axis vents ranging from 0.015 to 0.03 Tmol/y. In addition, Guzmán-Marmolejo et al. (7) and Kasting (8) determined abiotic CH₄ fluxes from hydrothermal systems ranging from 0.1 to 0.4 Tmol/y at present, and Kasting (8) found that this flux may potentially have been larger during the Hadean, ~1.5 Tmol/y, but this is still over an order of magnitude smaller than the current biogenic flux. Brovarone et al. (76) and Fiebig et al. (77) estimated abiotic hydrothermal CH₄ fluxes at subduction zones, finding modern fluxes of ~10⁻² Tmol/y similar to the above estimates. In continental settings, abiotic methane has been reported in low-temperature environments such as orogenic massifs and intrusions, seeps, crystalline shields, and ophiolites, with serpentinization of (iron-bearing) peridotites being the major source of methane in these settings (Fig. 2) (78). However, the amount of abiotic methane generated in continental settings is several orders of magnitude smaller than the biogenic flux (78–82).

Experimental studies on abiotic CH₄ production via water–rock and metamorphic reactions have also been conducted. The availability of H₂, the amount of excess aqueous carbonates, and the presence of mineral catalysts can greatly affect the amount of CH₄ generated experimentally (83, 84). While Oze et al. (84) and Neubeck et al. (85) found that CH₄ production by serpentinization is enhanced by the presence of mineral catalysts (e.g., chromite, magnetite, and awaruite), McCollom (71) cautions that

these experimental studies did not quantify their organic contamination. McCollom (86) used isotopic labeling to differentiate CH₄ produced by serpentinization from background sources. McCollom (86) found abiotic CH₄ formation via serpentinization to be extremely limited, with most of the experimentally generated CH₄ deriving from background sources. While iron oxidation and FTT-type reactions (or their metamorphic equivalents) are the most commonly discussed mechanisms for large abiotic fluxes on terrestrial planets, other possible mechanisms for reducing carbon include direct carbonate methanation and hydration of graphite-carbonate-bearing rocks, but they are also unlikely to generate false-positive scenarios (*SI Appendix, section 2*).

The critical limitation of hydrothermal CH₄ production is the supply of Fe²⁺ and the efficiency with which iron can be oxidized to generate CH₄. The availability of iron and the efficiency of its oxidation on a planetary scale depend on a range of geological and geochemical processes that operate across disparate spatial and temporal scales. Tectonic regime, mineral catalysis, volatile inventories, surface climate, and crustal composition and permeability/porosity all potentially modulate the efficiency and extent of crustal hydration. To investigate this process's limitations, Krissansen-Totton et al. (14) estimated the maximum CH₄ flux generated via serpentinization by exploring plausible ranges of parameters including crustal production rate, the fraction of FeO in fresh crust, the maximum fractional conversion of FeO to H₂ via serpentinization, and the maximum fractional conversion of H₂ to CH₄ via FTT reactions. Producing a probability distribution for the maximum abiotic CH₄ flux, they found that Earth-like biological CH₄ fluxes are at least an order of magnitude larger than plausible abiotic fluxes from serpentinization, consistent with the findings of the studies discussed above (14) (Fig. 4).

Ultimately, abiotic CH₄ generation via low-temperature water–rock or metamorphic reactions is unlikely to produce atmospheric CH₄ fluxes comparable to modern biotic fluxes in combination with atmospheric CO₂ (*SI Appendix, Table S2*

and Fig. 4). In fact, all CH₄ flux extrapolations from low-temperature system studies discussed above are consistent with the maximum abiotic flux estimates in ref. 14. Nevertheless, the possible parameter space for crustal methane production is vast, and work remains to be done to determine whether unfamiliar environmental conditions may exist on other planets that could produce a false-positive signal. For example, Fe-enriched olivine may be more common compositions for the mantles of other rocky planets compared to the Mg-rich olivine characteristic of Earth's mantle. McCollom et al. (87) determined that serpentinization of Fe-rich olivine can generate significantly more H₂ compared to that of Mg-rich olivine (by a factor of ~2 to 10) (87). Another source of uncertainty is what catalysts might be available in natural settings. At temperatures ≤600 K, in gas mixtures with CO₂ and H₂, CH₄ is thermodynamically preferred, but the reaction is kinetically inhibited and will proceed only if catalyzed. Future investigations could seek to develop coupled geochemical evolution models of a planet's mantle and crust that can self-consistently predict CH₄, CO₂, and CO fluxes from high-temperature magmatic processes and low-temperature hydrothermal and metamorphic systems, such that the contextual clues of abiotic methane can be explored for different compositional assumptions.

Impacts. The solar system terrestrial planets likely experienced a late-accreting veneer from impacts of comets and asteroids prior to 3.8 Ga (88). Impact events are plausible abiotic sources that can generate methane in two ways: 1) After a cometary impactor hits a planet, it vaporizes, and in the cooling impactor, some of the molecules delivered by the impactor may react to form CH₄ (89); and 2) large asteroid impactors could deliver a reducing power (i.e., iron) and vaporize a planet's surface ocean, causing a steam atmosphere to form, and CH₄ may form in such a cooling steam atmosphere (41). To generate significant methane, impact events require either a large, constant flux of impactors (case 1) or a transient postimpact atmosphere from a giant impact event (case 2).

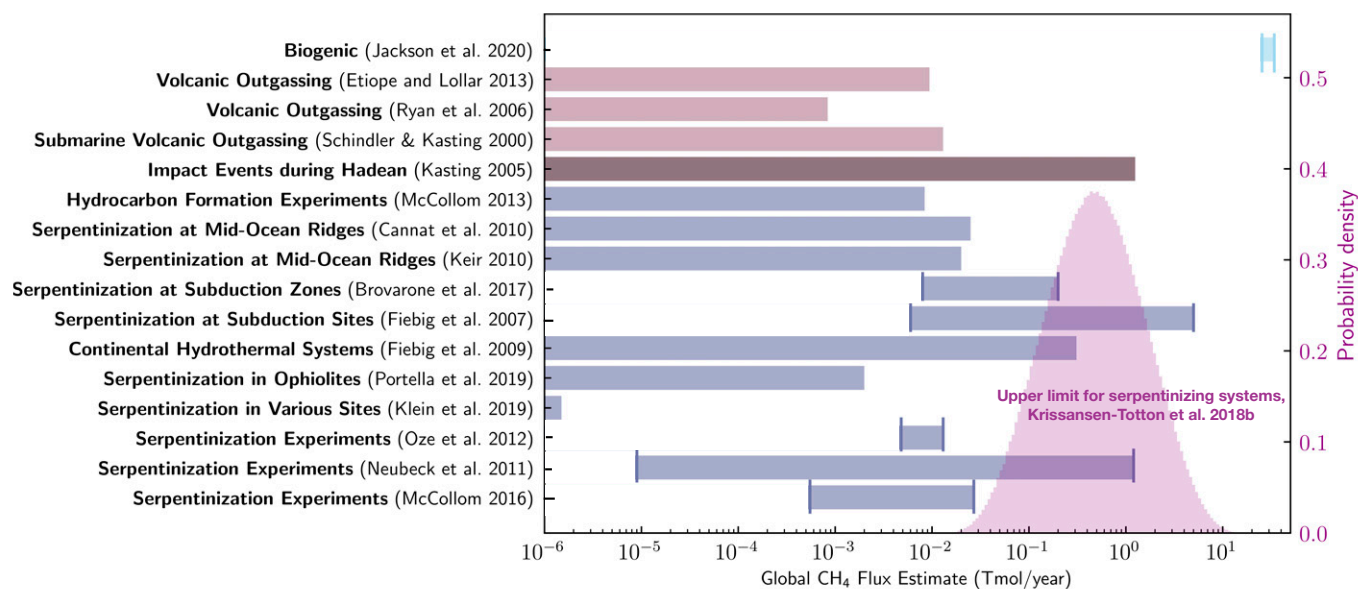


Fig. 4. Summary of known abiotic CH₄ sources with their estimated global CH₄ flux values compared to Earth's current biogenic CH₄ flux. As in *SI Appendix, Table S2*, for each abiotic source considered, we present those sources for which we can estimate global CH₄ flux values from a given reference. In the cases where there are multiple global CH₄ flux estimates for a given reference of an abiotic source, we show the maximum and minimum CH₄ flux estimates by the vertical lines (6, 8, 10, 14, 28, 58, 71, 73, 74, 76, 77, 79, 81, 82, 84–86). The transparent purple probability distribution for the maximum abiotic CH₄ flux from serpentinization is from ref. 14, and the right-hand y axis shows the probability density of this distribution. None of the abiotic sources considered have estimated global CH₄ fluxes that are similar to or exceed Earth's modern biogenic CH₄ flux. In fact, most of the abiotic sources have predicted global CH₄ fluxes that are at least an order of magnitude less than Earth's biogenic CH₄ flux. We do not show the flux estimates that exceed the iron supply because such extremely large fluxes are based on experimental results for which there are issues with organic contamination (main text).

For case 1, Kress and McKay (89) and Kasting (8) modeled CH_4 formation from volatile-rich impactors. Ref. 89 found that a 1-km comet can generate 0.6 Tmol of atmospheric CH_4 per impact event, and ref. 8 estimated that the global CH_4 impact flux during the Hadean was ~ 1.25 Tmol/y. However, it is unknown whether condensing dust from cometary impactors has effective catalytic properties to enable CH_4 generation. Recent theoretical and experimental work investigated the outgassing compositions of chondritic materials that may represent cometary impactors and found that there are small to negligible amounts of outgassed CH_4 from some of the most volatile-rich chondrites (i.e., CM chondrites) (90, 91).

For case 2, Zahnle et al. (41) showed that a transient reducing atmosphere (rich in CH_4 , H_2 , and NH_3) could have been generated on the early Earth by large asteroid impacts during the late-accreting veneer. Such giant impacts would produce methane since they delivered metallic iron, a significant reducing power, to the surface (41). The iron could react with Earth's existing H_2O to produce H_2 and FeO , which would subsequently react with atmospheric CO_2 or CO to produce CH_4 . The amount of methane that could form depends on the amount of carbon available prior to the impact, how much iron the impactor delivers, how much of that iron reacts with the atmosphere, and the presence of catalysts that can reduce the quench temperature so methane is thermodynamically stable (41). A possible false-positive scenario is one in which a giant impact event could produce a transient atmosphere with abundant CH_4 and CO_2 but low CO . However, calculations of transient impact-generated atmospheres of ref. 41 suggest that such false-positive scenarios are unlikely to be long lived for significant portions of geologic time and would be accompanied by H_2 -dominated atmospheres (e.g., figures 7, 8, and 12 in ref. 41).

Methane Beyond Earth: Mars and Temperate Exo-Titans.

Methane exists in other locations besides Earth throughout the solar system, including in the atmospheres of the outer planets and in comets (92). While super-Earths and sub-Neptune planets do not exist in our solar system, they are common among other planetary systems, and future studies could determine the surface pressures necessary for these planets to sustain methane via thermochemical recombination, without the need for a significant surface flux (*SI Appendix, section 5*). For example, if atmospheric H_2 is abundant, then CH_4 will efficiently recombine after photolysis, which dramatically increases the CH_4 lifetime (*SI Appendix, section 3*). As the focus of this study is on terrestrial planets, this section discusses atmospheric methane sources in other terrestrial worlds, in particular Mars and temperate Titan-like exoplanets (exo-Titans).

Mars. The presence of methane on Mars is debated, with claims of detections at the ~ 10 to 60 ppbv level that are highly variable in time and space by the European Space Agency's (ESA) Mars Express, NASA's Curiosity rover, and ground-based observations (52, 93, 94, 95). However, the most recent and most sensitive measurements by the ESA-Roscosmos ExoMars Trace Gas Orbiter did not detect any significant methane over all observed latitudes and reported an upper limit of ~ 20 ppt methane for altitudes above a few kilometers, several orders of magnitude lower than all previous purported CH_4 detections (96). Regardless, methane detections of a few parts per billion to tens of parts per billion are much lower than the terrestrial exoplanet thresholds for biogenic CH_4 considered in this study. There are a variety of plausible abiotic explanations for methane on Mars, including water-rock reactions, the release of clathrates, and degradation of organic matter.

Temperate exo-Titans. Methane exists (at ~ 1 to 5%) in the N_2 -rich atmosphere of Saturn's largest moon Titan (97). Photochemical models predict that the current CH_4 in Titan's atmosphere would be destroyed in ~ 30 My unless there is a mechanism that resupplies CH_4 to the atmosphere (98, 99). Possible mechanisms for Titan's CH_4 resupply include its subsurface ocean, CH_4 clathrate hydrates in the crust, liquid hydrocarbons in the subsurface, or outgassing from the interior (100). While life has been suggested as a possible explanation (101), the absence of conventionally habitable surface conditions makes geochemical processes more attractive explanations.

Whatever the source of Titan's methane, temperate Titan-like exoplanets are unlikely to produce a $\text{CH}_4 + \text{CO}_2$ biosignature false positive. We estimate the atmospheric CH_4 lifetime for an Earth-sized exoplanet with a Titan-like volatile inventory that migrates to the habitable zone where all surface ice melts (see *SI Appendix, section 6D* for a scenario where ice remains). Given initial CH_4 and CO_2 reservoirs relative to H_2O based on Titan's volatile inventory (102), we neglect oxidation via OH to be conservative and calculate the loss of CH_4 via diffusion-limited hydrogen escape (103). We assume that the atmospheric mixing ratio of CH_4 is 10%, which is conservative given the respective solubilities of CH_4 and CO_2 and plausible background N_2 inventories (*SI Appendix, section 6D*). We find that for planets with water mass fractions that are < 1.0 wt% of the planet's mass, the atmospheric CH_4 lifetime is short at habitable-zone separations (less than ~ 10 My) (Fig. 5). If the water mass fraction is ~ 10 wt% of the planet's mass, then atmospheric CH_4 may last for longer periods of time (~ 100 My), but even so the duration is much shorter than typical stellar ages. In any case, it will likely be possible to identify planets with such large water inventories via their low densities. Whether hydrogen's removal timescale could be dramatically lengthened via low loss rates or other large hydrogen reservoirs (while maintaining a CO_2 -rich atmosphere) is a promising topic for future computational studies.

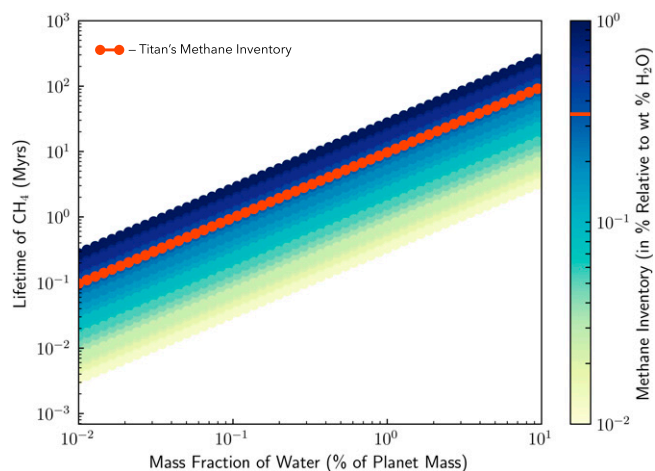


Fig. 5. The photochemical lifetime of methane biosignature false positives produced by melting volatile-rich Titan analogs is short. Shown is the estimated lifetime of atmospheric methane as a function of the planet's water mass and initial methane volatile inventory. Assuming methane's escape rate is diffusion limited and that its steady-state mixing ratio is 10%, we varied the initial methane volatile inventory (drawing values from a uniform distribution from 0.01 to 1.0% relative to weight % water, represented by the color bar) and the mass fraction of the planet's water (exploring values from 0.01 to 10% of the mass of the planet, assuming an Earth-mass planet) and calculated the estimated lifetime for methane in the atmosphere (*SI Appendix, section 6D*). The red curve represents Titan's methane inventory ($\sim 0.35\%$) (102). For planets with Titan-like methane inventories and water mass fractions that are 1% (10%) of the planet's mass, the lifetime of atmospheric methane will be ~ 10 My (~ 100 My).

Discussion

Toward Procedures to Identify Methane Biosignatures. Any procedure for observationally identifying methane biosignatures must take into account the broader planetary and astrophysical context and will be dictated by the capabilities of the available instruments. Major steps might include the following: 1) detecting a terrestrial planet within the habitable zone of its host star and characterizing its bulk properties (e.g., mass, radius, orbital properties); 2) measuring its atmospheric composition, namely the abundances of CH₄, CO₂, CO, H₂O, and H₂ and confirming that the atmosphere is anoxic; and 3) identifying possible false positives and combining this information with observational data on the planet's broader context to determine the likelihood of abiotic vs. biotic sources of methane (*SI Appendix, Fig. S3*). It is important that the host star is well characterized (i.e., UV radiation and stellar activity) to understand the planet's photochemical environment. Identifying the presence of liquid water on the surface of a planet would suggest a particularly compelling target since it is a likely requirement for life.

Constraining the atmospheric abundances of CH₄, CO₂, and CO and confirming that the atmosphere is not H₂ dominated is essential for determining whether the planet's atmosphere is indicative of the presence of a biosphere. Terrestrial planets with high mean-molecular-weight atmospheres are better candidates to search for methane biosignatures because in such atmospheres, the CH₄ lifetime will be very short without a significant replenishment source. In addition, confirming that the planet's atmosphere is anoxic is necessary to distinguish a false-positive case for an anoxic planet with abundant atmospheric CH₄, CO₂, and CO from an oxic planet with an oxygen-based biosphere that has atmospheric CH₄, CO₂, CO, and O₂ (37). With these abundances constrained, a photochemical model can infer the surface fluxes of the atmospheric constituents. Indications that these surface fluxes may be consistent with a biosphere include large implied CH₄ fluxes coexisting with atmospheric CO₂ but comparatively low CO abundances.

Even if the surface fluxes are consistent with a biosphere, it is necessary to identify all possible false positives including magmatic outgassing from a reduced mantle (Fig. 3), water–rock and metamorphic reactions (Fig. 4), large impact fluxes, and large volatile inventories (Fig. 5). The viability of detecting methane biosignatures depends on our knowledge of abiotic methane sources and their production rates. One of the most outstanding uncertainties is an incomplete understanding of plausible abiotic methane production on a planetary scale via water–rock and metamorphic reactions. If a planet has an atmospheric composition consistent with a methanogenic biosphere but false positives cannot be entirely ruled out, it will be necessary to search for corroborating evidence such as additional biosignature gases [e.g., methyl chloride (46), organosulfur compounds (104)], signs of atmospheric seasonality, and reflectance signatures from pigmented surface organisms (105, 106) (*SI Appendix, Fig. S3*). Ultimately, definitively detecting the presence of methane biosignatures on a terrestrial exoplanet will require taking into account the entire planetary and astrophysical context, characterizing the planet's atmospheric composition, investigating all potential false-positive scenarios, and likely searching for supporting evidence.

Detectability Prospects. Prospects for detecting biogenic levels of methane in terrestrial exoplanet atmospheres in the near future with JWST are promising (17, 24, 25, 27). However, it may be challenging to obtain sufficient observational data on the planetary context to confirm the presence of methane

biosignatures and rule out false positives. Although JWST may be able to detect CO₂, it will provide only crude constraints on CO abundances (17, 27). Ref. 27 determined that JWST could place upper bounds on CO abundances in ~10 transits and constrain the CO/CH₄ ratio with more transits for an Archean Earth-like TRAPPIST-1e (27). Ref. 17 confirms that JWST will likely be able to crudely constrain the CO/CH₄ ratio and notes that CO constraints will be possible with high-resolution spectroscopy measurements with extremely large telescopes (ELTs). If biospheres are dominated by oxygenic photosynthesis, they may produce large CO fluxes through biomass burning (37). Therefore, to distinguish an anoxic, lifeless world with abundant atmospheric CH₄, CO₂, and CO from an oxic, inhabited planet with CH₄, CO₂, CO, and O₂ requires observations that can detect or rule out the presence of atmospheric O₂/O₃, which will be challenging with JWST (37). In addition, JWST will not be able to detect water vapor with transit observations due to water cloud condensation nor constrain surface properties, so it will not be able to fully assess habitability (107, 108). Nevertheless, if JWST detects significant CH₄ and CO₂ and places some constraints on the CO/CH₄ ratio in a terrestrial exoplanet's atmosphere, such a discovery would certainly motivate observations with future instruments.

Looking ahead, ground-based ELTs will help characterize terrestrial exoplanets and their biosignatures (109). Ref. 26 determined that for a cloud-free, low-CO₂ TRAPPIST-1e atmosphere, a mere 10 ppm CH₄ is likely detectable with high-resolution transit spectroscopy with the European ELT in less than ~30 transits, and CO detections may be possible with ~40 transits (26). In addition, the Astro2020 Decadal Survey recommended an ~6m infrared/optical/UV space telescope to characterize the atmospheres of dozens of habitable-zone terrestrial exoplanets, including detecting methane (5, 110). Identifying methane biosignatures will require not only detecting and constraining the atmospheric abundances of CH₄, CO₂, and CO, but also using a combination of observational tools to comprehensively characterize the broader planetary context.

Conclusions

With the upcoming technological advancements in exoplanet observations enabling the characterization of potentially habitable exoplanets, it is important to consider possible biosignature gases and the sources of false-positive detections. This is particularly urgent for methane since biogenic methane is likely detectable for some terrestrial exoplanets with JWST. The case for methane as a biosignature stems from the fact that photochemistry of terrestrial planet atmospheres implies that large CH₄ surface fluxes are required to sustain high levels of atmospheric methane. Although a variety of abiotic mechanisms could, under diverse planetary environments, replenish atmospheric methane, we find that it is challenging for such sources to produce abiotic CH₄ fluxes comparable to Earth's biogenic flux without also generating observable contextual clues that would signify a false positive. For example, we investigated whether planets with very reduced mantles and crusts can generate large methane fluxes via magmatic outgassing and assessed the existing literature on low-temperature water–rock and metamorphic reactions and, where possible, determined their maximum global abiotic methane fluxes. In every case, abiotic processes cannot easily produce atmospheres rich in both CH₄ and CO₂ with negligible CO due to the strong redox disequilibrium between CO₂ and CH₄ and the fact that CO is expected to be readily consumed by life. We also explored whether habitable-zone exoplanets that have large volatile inventories like

Titan could have long lifetimes of atmospheric methane. We found that, for Earth-mass planets with water mass fractions that are less than ~1% of the planet's mass, the lifetime of atmospheric methane is less than ~10 My, and observational tools can likely distinguish planets with larger water mass fractions from those with terrestrial densities.

Clearly, the mere detection of methane in an exoplanet's atmosphere is not sufficient evidence to indicate the presence of life given the variety of abiotic methane-production mechanisms. Instead, the entire planetary and astrophysical context must be taken into account to interpret atmospheric methane. *SI Appendix, Fig. S3* illustrates a tentative procedure for identifying methane biosignatures in the atmospheres of habitable terrestrial exoplanets. Ultimately, methane is more likely to be biogenic on a habitable-zone planet when 1) planet bulk density is terrestrial (no large surface volatile reservoirs), the atmosphere has a high mean molecular weight and is anoxic, and the host star is old; 2) the atmospheric CH₄ abundance is high, with implied surface replenishment fluxes exceeding what could plausibly be produced by known abiotic processes (~10 Tmol/y); and 3) when atmospheric methane is accompanied by CO₂ but comparatively little CO (or CO/CH₄ < 1).

Materials and Methods

We use the photochemical model PhotochemPy in *SI Appendix, Fig. S1* (*SI Appendix, section 6A*). The calculations for determining how carbon partitions

between different phases under various redox conditions for Fig. 3 follow the methods in ref. 63 and are discussed further in *SI Appendix, section 6B*. The global abiotic CH₄ flux estimates in Fig. 4 are described in detail in *SI Appendix, section 6C*. For Fig. 5, we estimate the atmospheric CH₄ lifetime for an Earth-mass terrestrial planet with different water mass fractions and Titan-like volatile inventories by assuming the escape flux of hydrogen is diffusion limited (*SI Appendix, section 6D*). The codes used for our analysis are available on GitHub at <https://github.com/maggiemagie/MethaneBiosignature> (*SI Appendix, section 6*).

Data Availability. All data needed to evaluate the conclusions in this paper are present in this paper and/or in *SI Appendix, Materials and Methods*. PhotochemPy can be accessed at GitHub (<https://github.com/Nicholaswogan/PhotochemPy>). Python code data have been deposited in GitHub (<https://github.com/maggiemagie/MethaneBiosignature>) (111).

ACKNOWLEDGMENTS. We thank James Kasting and the other anonymous reviewer for constructive reviews. We thank David Catling, Edward Schwieterman, Xinting Yu, Kevin Zahnle, and Stephanie Olson for helpful discussions and comments. We thank Elena Hartley (<http://www.elabarts.com>) for creating Fig. 2. J.K.-T. is supported by the NASA Sagan Fellowship and through the NASA Hubble Fellowship Grant HF2-51437 awarded by the Space Telescope Science Institute, which is operated by the Association of Universities for Research in Astronomy, Inc., for NASA, under Contract NAS5-26555. N.W. is supported by the NASA Astrobiology Program Grant 80NSSC18K0829. N.M.T. is supported by NASA Emerging Worlds Grant 80NSSC18K0498 and NASA Planetary Science Early Career Award Grant 80NSSC20K1078. M.A.T., M.T., and J.F.F. are supported by NASA under Award 19-ICAR19-2-0041.

1. M. Gillon *et al.*, Seven temperate terrestrial planets around the nearby ultracool dwarf star TRAPPIST-1. *Nature* **542**, 456–460 (2017).
2. C. V. Morley, L. Kreidberg, Z. Rustamkulov, T. Robinson, J. J. Fortney, Observing the atmospheres of known temperate Earth-sized planets with JWST. *Astrophys. J.* **850**, 121 (2017).
3. R. Gilmozzi, J. Spyromilio, The European extremely large telescope (E-ELT). *Messenger (Los Angel.)* **127**, 9 (2007).
4. M. López-Morales *et al.*, Optimizing ground-based observations of O₂ in Earth analogs. *Astron. J.* **158**, 15 (2019).
5. F. A. Harrison *et al.*, *Pathways to Discovery in Astronomy and Astrophysics for the 2020s*, National Academies Press, Ed. (National Academies of Science, Engineering and Medicine, Washington, DC, 2021).
6. T. L. Schindler, J. F. Kasting, Synthetic spectra of simulated terrestrial atmospheres containing possible biomarker gases. *Icarus* **145**, 262–271 (2000).
7. A. Guzmán-Marmolejo, A. Segura, E. Escobar-Briones, Abiotic production of methane in terrestrial planets. *Astrobiology* **13**, 550–559 (2013).
8. J. F. Kasting, Methane and climate during the Precambrian era. *Precambrian Res.* **137**, 119–129 (2005).
9. D. J. Des Marais *et al.*, Remote sensing of planetary properties and biosignatures on extrasolar terrestrial planets. *Astrobiology* **2**, 153–181 (2002).
10. G. Etiope, B. S. Lollar, Abiotic methane on Earth. *Rev. Geophys.* **51**, 276–299 (2013).
11. N. Wogan, J. Krissansen-Totton, D. C. Catling, Abundant atmospheric methane from volcanism on terrestrial planets is unlikely and strengthens the case for methane as a biosignature. *Planet. Sci. J.* **1**, 58 (2020).
12. J. E. Lovelock, Thermodynamics and the recognition of alien biospheres. *Proc. R. Soc. Lond. B Biol. Sci.* **189**, 167–180 (1975).
13. E. Simoncini, N. Virgo, A. Kleidon, Quantifying the drivers of chemical disequilibrium: Theory and application to methane in Earth's atmosphere. *Earth Syst. Dyn.* **4**, 317–331 (2013).
14. J. Krissansen-Totton, S. Olson, D. C. Catling, Disequilibrium biosignatures over Earth history and implications for detecting exoplanet life. *Sci. Adv.* **4**, eaao5747 (2018).
15. E. W. Schwieterman *et al.*, Exoplanet biosignatures: A review of remotely detectable signs of life. *Astrobiology* **18**, 663–708 (2018).
16. G. Arney, S. D. Domagal-Goldman, V. S. Meadows, Organic haze as a biosignature in anoxic Earth-like atmospheres. *Astrobiology* **18**, 311–329 (2018).
17. T. Mikal-Evans, Detecting the proposed CH₄-CO₂ biosignature pair with the James Webb Space Telescope: TRAPPIST-1e and the effect of cloud/haze. *Mon. Not. R. Astron. Soc.* **510**, 980–991 (2021).
18. D. C. Catling, K. J. Zahnle, C. McKay, Biogenic methane, hydrogen escape, and the irreversible oxidation of early Earth. *Science* **293**, 839–843 (2001).
19. D. C. Catling, K. J. Zahnle, The Archean atmosphere. *Sci. Adv.* **6**, eaax1420 (2020).
20. V. S. Meadows *et al.*, Exoplanet biosignatures: Understanding oxygen as a biosignature in the context of its environment. *Astrobiology* **18**, 630–662 (2018).
21. C. Sousa-Silva *et al.*, Phosphine as a biosignature gas in exoplanet atmospheres. *Astrobiology* **20**, 235–268 (2020).
22. Z. Zhan *et al.*, Assessment of isoprene as a possible biosignature gas in exoplanets with anoxic atmospheres. *Astrobiology* **21**, 765–792 (2021).
23. J. Huang *et al.*, Assessment of ammonia as a biosignature gas in exoplanet atmospheres. *Astrobiology* **22**, 1–58 (2022).
24. M. T. Gialluca, T. D. Robinson, S. Rugheimer, F. Wunderlich, Characterizing atmospheres of transiting Earth-like exoplanets orbiting M dwarfs with James Webb Space Telescope. *Publ. Astron. Soc. Pac.* **133**, 054401 (2021).
25. F. Wunderlich *et al.*, Detectability of atmospheric features of Earth-like planets in the habitable zone around M dwarfs. *Astron. Astrophys.* **624**, A49 (2019).
26. F. Wunderlich *et al.*, Distinguishing between wet and dry atmospheres of TRAPPIST-1 e and f. *Astrophys. J.* **901**, 126 (2020).
27. J. Krissansen-Totton, R. Garland, P. Irwin, D. C. Catling, Detectability of biosignatures in anoxic atmospheres with the James Webb Space Telescope: A TRAPPIST-1e case study. *Astron. J.* **156**, 13 (2018).
28. R. B. Jackson *et al.*, Increasing anthropogenic methane emissions arise equally from agricultural and fossil fuel sources. *Environ. Res. Lett.* **15**, 7 (2020).
29. Z. Lyu, N. Shao, T. Akinyemi, W. B. Whitman, Methanogenesis. *Curr. Biol.* **28**, R727–R732 (2018).
30. J. M. Wolfe, G. P. Fournier, Horizontal gene transfer constrains the timing of methanogen evolution. *Nat. Ecol. Evol.* **2**, 897–903 (2018).
31. F. U. Battistuzzi, A. Feijao, S. B. Hedges, A genomic timescale of prokaryote evolution: Insights into the origin of methanogenesis, phototrophy, and the colonization of land. *BMC Evol. Biol.* **4**, 44 (2004).
32. M. C. Weiss *et al.*, The physiology and habitat of the last universal common ancestor. *Nat. Microbiol.* **1**, 16116 (2016).
33. K. J. Zahnle, M. Gacesa, D. C. Catling, Strange messenger: A new history of hydrogen on Earth, as told by xenon. *Geochim. Cosmochim. Acta* **244**, 56–85 (2019).
34. S. Kadoya, D. C. Catling, Constraints on hydrogen levels in the Archean atmosphere based on detrital magnetite. *Geochim. Cosmochim. Acta* **262**, 207–219 (2019).
35. P. Kharcha, J. Kasting, J. Siefert, A coupled atmosphere-ecosystem model of the early Archean Earth. *Geobiology* **3**, 53–76 (2005).
36. K. Ozaki, E. Tajika, P. K. Hong, Y. Nakagawa, C. T. Reinhard, Effects of primitive photosynthesis on Earth's early climate system. *Nat. Geosci.* **11**, 55–59 (2017).
37. E. W. Schwieterman *et al.*, Rethinking CO antibiosignatures in the search for life beyond the solar system. *Astrophys. J.* **874**, 10 (2019).
38. B. Sauterey, B. Charnay, A. Affholder, S. Mazevet, R. Ferrière, Co-evolution of primitive methane-cycling ecosystems and early Earth's atmosphere and climate. *Nat. Commun.* **11**, 2705 (2020).
39. T. A. Laakso, D. P. Schrag, Methane in the Precambrian atmosphere. *Earth Planet. Sci. Lett.* **522**, 48–54 (2019).
40. T. M. Lenton, On the use of models in understanding the rise of complex life. *Interface Focus* **10**, 20200018 (2020).
41. K. J. Zahnle, R. Lupu, D. C. Catling, N. Wogan, Creation and evolution of impact-generated reduced atmospheres of early Earth. *Planet. Sci. J.* **1**, 11 (2020).
42. G. Arney *et al.*, The pale orange dot: The spectrum and habitability of hazy Archean Earth. *Astrobiology* **16**, 873–899 (2016).
43. N. Wogan, PhotochemPy v0.1.0. Zenodo. <https://doi.org/10.5281/zenodo.6360737> (2022).
44. R. G. Priin *et al.*, Evidence for substantial variations of atmospheric hydroxyl radicals in the past two decades. *Science* **292**, 1882–1888 (2001).
45. J. F. Kasting, L. L. Brown, Methane concentrations in the Earth's prebiotic atmosphere. *Orig. Life Evol. Biosph.* **26**, 2 (1996).
46. A. Segura *et al.*, Biosignatures from Earth-like planets around M dwarfs. *Astrobiology* **5**, 706–725 (2005).

47. S. L. Olson, C. T. Reinhard, T. W. Lyons, Limited role for methane in the mid-Proterozoic greenhouse. *Proc. Natl. Acad. Sci. U.S.A.* **113**, 11447–11452 (2016).
48. J. Krissansen-Totton, D. S. Bergsman, D. C. Catling, Thermodynamic disequilibrium in planetary atmospheres. *Astrobiology* **16**, 39–67 (2016).
49. A. A. Pavlov, L. L. Brown, J. F. Kasting, UV shielding of NH₃ and O₂ by organic hazes in the Archean atmosphere. *J. Geophys. Res.* **106**, 23267–23288 (2001).
50. J. F. Kasting, L. L. Brown, "The early atmosphere as a source of biogenic compounds" in *The Molecular Origins of Life: Assembling Pieces of the Puzzle*, A. Brack, Ed. (Cambridge University Press, 1998), pp. 35–56.
51. S. F. Sholes, J. Krissansen-Totton, D. C. Catling, A maximum subsurface biomass on Mars from untapped free energy: CO and H₂ as potential antibioticsignatures. *Astrobiology* **19**, 655–668 (2019).
52. K. Zahnle, R. S. Freedman, D. C. Catling, Is there methane on Mars? *Icarus* **212**, 493–503 (2011).
53. S. W. Ragsdale, Life with carbon monoxide. *Crit. Rev. Biochem. Mol. Biol.* **39**, 165–195 (2004).
54. J. G. Ferry, C. H. House, The stepwise evolution of early life driven by energy conservation. *Mol. Biol. Evol.* **23**, 1286–1292 (2006).
55. D. J. Lessner *et al.*, An unconventional pathway for reduction of CO₂ to methane in CO-grown *Methanosarcina acetivorans* revealed by proteomics. *Proc. Natl. Acad. Sci. U.S.A.* **103**, 17921–17926 (2006).
56. S. M. Techtmann, A. S. Colman, F. T. Robb, 'That which does not kill us only makes us stronger': The role of carbon monoxide in thermophilic microbial consortia. *Environ. Microbiol.* **11**, 1027–1037 (2009).
57. J. H. Jeoung, H. Dobbek, Carbon dioxide activation at the Ni,Fe-cluster of anaerobic carbon monoxide dehydrogenase. *Science* **318**, 1461–1464 (2007).
58. S. Ryan, E. J. Dlugokencky, P. P. Tans, M. E. Trudeau, Mauna Loa volcano is not a methane source: Implications for Mars. *Geophys. Res. Lett.* **33**, L12301 (2006).
59. W. D. Huff, L. A. Owen, "Volcanic landforms and hazards" in *Treatise on Geomorphology*, L. A. Owen, Ed. (Elsevier, 2013), vol. 5, pp. 148–192.
60. G. Etiope, A. Feyzullayev, C. L. Baciu, Terrestrial methane seeps and mud volcanoes: A global perspective of gas origin. *Mar. Pet. Geol.* **26**, 333–344 (2009).
61. O. Namur, B. Charlier, F. Holtz, C. Cartier, C. McCammon, Sulfur solubility in reduced mafic silicate melts: Implications for the speciation and distribution of sulfur on mercury. *Earth Planet. Sci. Lett.* **448**, 102–114 (2016).
62. P. N. Peplowski *et al.*, Remote sensing evidence for an ancient carbon-bearing crust on Mercury. *Nat. Geosci.* **9**, 273–276 (2016).
63. G. Ortenzi *et al.*, Mantle redox state drives outgassing chemistry and atmospheric composition of rocky planets. *Sci. Rep.* **10**, 10907 (2020).
64. C. M. Guimond, L. Noack, G. Ortenzi, F. Sohl, Low volcanic outgassing rates for a stagnant lid Archean Earth with graphite-saturated magmas. *Phys. Earth Planet. Inter.* **320**, 15 (2021).
65. M. M. Hirschmann, A. C. Withers, Ventilation of CO₂ from a reduced mantle and consequences for the early Martian greenhouse. *Earth Planet. Sci. Lett.* **270**, 147–155 (2008).
66. A. E. Doyle, E. D. Young, B. Klein, B. Zuckerman, H. E. Schlichting, Oxygen fugacities of extrasolar rocks: Evidence for an Earth-like geochemistry of exoplanets. *Science* **366**, 356–359 (2019).
67. E. Cottrell, K. A. Kelley, The oxidation state of Fe in orb glasses and the oxygen fugacity of the upper mantle. *Earth Planet. Sci. Lett.* **305**, 270–282 (2011).
68. S. Kadoya, D. C. Catling, R. W. Nicklas, I. S. Puchtel, A. D. Anbar, Mantle data imply a decline of oxidizable volcanic gases could have triggered the Great Oxidation. *Nat. Commun.* **11**, 2774 (2020).
69. T. M. McCollom, W. Bach, Thermodynamic constraints on hydrogen generation during serpentinization of ultramafic rocks. *Geochim. Cosmochim. Acta* **73**, 856–875 (2009).
70. T. M. McCollom, J. S. Seewald, A reassessment of the potential for reduction of dissolved CO₂ to hydrocarbons during serpentinization of olivine. *Geochim. Cosmochim. Acta* **65**, 3769–3778 (2001).
71. T. M. McCollom, Laboratory simulations of abiotic hydrocarbon formation in Earth's deep subsurface. *Rev. Mineral. Geochem.* **75**, 467–494 (2013).
72. T. M. McCollom, Formation of meteorite hydrocarbons from thermal decomposition of siderite (FeCO₃). *Geochim. Cosmochim. Acta* **67**, 311–317 (2003).
73. R. S. Keir, A note on the fluxes of abiogenic methane and hydrogen from mid-ocean ridges. *Geophys. Res. Lett.* **37**, L24609 (2010).
74. M. Cannat, F. Fontaine, J. Escartin, "Serpentinization and associated hydrogen and methane fluxes at slow spreading ridges" in *Diversity of Hydrothermal Systems on Slow Spreading Ocean Ridges*, P. A. Rona, C. W. Devey, J. Dymert, B. J. Murton, Eds. (American Geophysical Union, 2010), vol. 188, pp. 241–264.
75. D. C. Catling, J. F. Kasting, *Atmospheric Evolution on Inhabited and Lifeless Worlds* (Cambridge University Press, 2017).
76. A. Vitale Brovarone *et al.*, Massive production of abiotic methane during subduction evidenced in metamorphosed ophiocarbonates from the Italian Alps. *Nat. Commun.* **8**, 14134 (2017).
77. J. Fiebig, A. B. Woodland, J. Spangenberg, W. Oschmann, Natural evidence for rapid abiogenic hydrothermal generation of CH₄. *Geochim. Cosmochim. Acta* **71**, 3028–3039 (2007).
78. G. Etiope, Abiotic methane in continental serpentinization sites: An overview. *Procedia Earth Planet. Sci.* **17**, 9–12 (2017).
79. J. Fiebig, A. B. Woodland, W. D'Alessandro, W. Püttmann, Excess methane in continental hydrothermal emissions is abiogenic. *Geology* **37**, 495–498 (2009).
80. R. Kietäväinen, L. Ahonen, P. Niinikoski, H. Nykänen, I. T. Kukkonen, Abiotic and biotic controls on methane formation down to 2.5 km depth within the Precambrian Fennoscandian shield. *Geochim. Cosmochim. Acta* **202**, 124–145 (2017).
81. Y. de Melo Portella, F. Zaccarini, G. Etiope, First detection of methane within chromitites of an Archean-paleoproterozoic greenstone belt in Brazil. *Minerals (Basel)* **9**, 15 (2019).
82. F. Klein, N. G. Grozeva, J. S. Seewald, Abiotic methane synthesis and serpentinization in olivine-hosted fluid inclusions. *Proc. Natl. Acad. Sci. U.S.A.* **116**, 17666–17672 (2019).
83. C. L. Jones, R. Rosenbauer, J. I. Goldsmith, C. Oze, Carbonate control of H₂ and CH₄ production in serpentinization systems at elevated P-Ts. *Geophys. Res. Lett.* **37**, L14306 (2010).
84. C. Oze, L. C. Jones, J. I. Goldsmith, R. J. Rosenbauer, Differentiating biotic from abiotic methane genesis in hydrothermally active planetary surfaces. *Proc. Natl. Acad. Sci. U.S.A.* **109**, 9750–9754 (2012).
85. A. Neubeck, N. T. Duc, D. Bastviken, P. Crill, N. G. Holm, Formation of H₂ and CH₄ by weathering of olivine at temperatures between 30 and 70°C. *Geochim. Trans.* **12**, 6 (2011).
86. T. M. McCollom, Abiotic methane formation during experimental serpentinization of olivine. *Proc. Natl. Acad. Sci. U.S.A.* **113**, 13965–13970 (2016).
87. T. M. McCollom, F. Klein, M. Ramba, Hydrogen generation from serpentinization of iron-rich olivine on Mars, icy moons, and other planetary bodies. *Icarus* **372**, 114754 (2022).
88. C. F. Chyba, Impact delivery and erosion of planetary oceans in the early inner solar system. *Nature* **343**, 129–133 (1990).
89. M. E. Kress, C. P. McKay, Formation of methane in comet impacts: Implications for Earth, Mars, and Titan. *Icarus* **168**, 475–483 (2004).
90. L. Schaefer, B. Fegley, Chemistry of atmospheres formed during accretion of the Earth and other terrestrial planets. *Icarus* **208**, 438–448 (2010).
91. M. A. Thompson *et al.*, Composition of terrestrial exoplanet atmospheres from meteorite outgassing experiments. *Nat. Astron.* **5**, 575–585 (2021).
92. A. Guzmán-Marmolejo, A. Segura, Methane in the solar system. *Bol. Soc. Geol. Mex.* **67**, 377–385 (2015).
93. V. Formisano, S. Atreya, T. Encrenaz, N. Ignatiev, M. Giuranna, Detection of methane in the atmosphere of Mars. *Science* **306**, 1758–1761 (2004).
94. M. J. Mumma *et al.*, Strong release of methane on Mars in northern summer 2003. *Science* **323**, 1041–1045 (2009).
95. C. R. Webster *et al.*, MSL Science Team, Mars atmosphere. Mars methane detection and variability at Gale crater. *Science* **347**, 415–417 (2015).
96. N. Thomas *et al.*, "The exoMars trace gas orbiter – First Martian year in orbit" in *43rd COSPAR Scientific Assembly*, R. Boyce, Ed. (The 43rd COSPAR Scientific Assembly, 2021), vol. 43, p. 149.
97. G. F. Lindal *et al.*, The atmosphere of Titan: An analysis of the Voyager 1 radio occultation measurements. *Icarus* **53**, 348–363 (1983).
98. Y. L. Yung, M. Allen, J. P. Pinto, Photochemistry of the atmosphere of Titan: Comparison between model and observations. *Astrophys. J. Suppl. Ser.* **55**, 465–506 (1984).
99. E. H. Wilson, S. K. Atreya, Current state of modeling the photochemistry of Titan's mutually dependent atmosphere and ionosphere. *J. Geophys. Res. Planets* **109**, E06002 (2004).
100. S. M. Hörst, Titan's atmosphere and climate. *J. Geophys. Res. Planets* **122**, 432–482 (2017).
101. C. P. McKay, H. D. Smith, Possibilities for methanogenic life in liquid methane on the surface of Titan. *Icarus* **178**, 274–276 (2005).
102. G. Tobie, D. Gautier, F. Hersant, Titan's bulk composition constrained by Cassini-Huygens: Implication for internal outgassing. *Astrophys. J.* **752**, 125 (2012).
103. D. C. Catling, J. F. Kasting, "Escape of atmospheres to space" in *Atmospheric Evolution on Inhabited and Lifeless Worlds*, D. C. Catling, J. F. Kasting, Ed. (Cambridge University Press, 2017), pp. 129–168.
104. S. D. Domagal-Goldman, V. S. Meadows, M. W. Claire, J. F. Kasting, Using biogenic sulfur gases as remotely detectable biosignatures on anoxic planets. *Astrobiology* **11**, 419–441 (2011).
105. S. L. Olson *et al.*, Atmospheric seasonality as an exoplanet biosignature. *Astrophys. J.* **858**, L14 (2018).
106. E. W. Schwieterman, C. S. Cockell, V. S. Meadows, Nonphotosynthetic pigments as potential biosignatures. *Astrobiology* **15**, 341–361 (2015).
107. T. D. Komacek, T. J. Faucher, E. T. Wolf, D. S. Abbot, Clouds will likely prevent the detection of water vapor in JWST transmission spectra of terrestrial exoplanets. *Astrophys. J.* **888**, L20 (2020).
108. T. J. Faucher *et al.*, Impact of clouds and hazes on the simulated JWST transmission spectra of habitable zone planets in the TRAPPIST-1 system. *Astrophys. J.* **887**, 194 (2019).
109. M. López-Morales *et al.*, Detecting Earth-like biosignatures on rocky exoplanets around nearby stars with ground-based extremely large telescopes. *Bull. Am. Astron. Soc.* **51**, 162 (2019).
110. TL Team, "The Luvuor mission concept study final report, (NASA)" (Tech. Rep., NASA Goddard Space Flight Center, Greenbelt, MD, 2019).
111. M. Thompson, J. Krissansen-Totton, N. Wogan, maggieapril3/MethaneBiosignature. GitHub. <https://github.com/maggieapril3/MethaneBiosignature>. Deposited 14 March 2022.



Supplementary Information for

The Case and Context for Atmospheric Methane as an Exoplanet Biosignature

Maggie A. Thompson, Joshua Krissansen-Totton, Nicholas Wogan, Myriam Telus, Jonathan J. Fortney

Maggie A. Thompson.
E-mail: maaphom@ucsc.edu

This PDF file includes:

Supplementary text
Figs. S1 to S3 (not allowed for Brief Reports)
Tables S1 to S3 (not allowed for Brief Reports)
SI References

Supporting Information Text

1. Atmospheres with Abundant CH₄ and CO₂ in Chemical Equilibrium—Discussion of Woitke et al. 2021

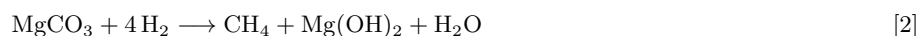
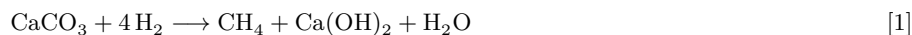
Could there be a biosignature false-positive scenario in which abundant CH₄ and CO₂ (without CO) coexist in thermochemical equilibrium in a rocky planet's atmosphere? Woitke et al. 2021 (1) show that at temperatures below ~600 K, CO₂, CH₄, N₂, and H₂O could coexist in chemical equilibrium if aqueous species are neglected. However, Woitke et al. 2021 (1) did not consider photochemistry and its effects on the stability of these atmospheres. Photochemistry is essential when assessing the plausibility of proposed terrestrial planet atmospheres.

To illustrate how a large CH₄ surface flux would be required to sustain high levels of atmospheric CH₄, a series of photochemical models were run simulating terrestrial planet atmospheres. We used PhotochemPy, a photochemical model adapted from the Atmos code (2) and created by N. Wogan ((3), <https://github.com/Nicholaswogan/PhotochemPy>), that uses a set of inputs (e.g., stellar flux, atmospheric temperature structure, chemical species and reactions) and then integrates the atmosphere forward in time until it reaches a photochemical steady state (see SI Section 6A). A series of models were generated assuming a planet with an initial atmospheric composition that is Archean Earth-like (i.e., N₂-CO₂-CH₄), orbiting a 2.7 Ga Sun-like star and explored a range of CO₂ and CH₄ surface mixing ratios from 0.1 to 0.5 and from 10⁻⁵ to 0.1, respectively.

Figure S1 illustrates that abundant atmospheric CH₄ in atmospheres containing CO₂, N₂, and H₂O, requires CH₄ surface fluxes similar to or greater than modern Earth's biogenic flux to balance photochemical destruction. Therefore, such an atmosphere will not be stable without a significant CH₄ replenishment source that likely exceeds Earth's modern biogenic flux. For example, in order to sustain high atmospheric CH₄ mixing ratios of ~0.1 along with significant amounts of CO₂, the required CH₄ surface fluxes are on the order of ~3.7 × 10¹² molecules/cm²/s (~1000 Tmol/year), corresponding to the yellow regions of Figure S1. Such a large CH₄ replenishment flux would be about 30 times larger than Earth's current biogenic flux (30 Tmol/year). Considering the global redox budget, such abundant atmospheric CH₄ requires that either the flux of reductants from Earth's interior is at least three orders of magnitude higher than Earth's modern hydrogen outgassing rate or that the H₂ escape rate is much less than the diffusion limit (4). In addition, the equilibrium calculations of (1) did not consider the formation of dissolved ammonium (NH₄⁺) and bicarbonate (HCO₃⁻), which are shown to be the equilibrium products of CO₂, CH₄, and N₂ in the presence of liquid water in (5). The thermochemical calculations of (1) could instead have relevance for deep sub-Neptune atmospheres.

2. Additional Water-Rock and Metamorphic Reactions and Key Unknowns

While iron oxidation and FTT-type reactions (or their metamorphic equivalents) are the most commonly discussed mechanisms for large abiotic fluxes on terrestrial planets (Figure 2), it is worth considering other possible mechanisms for reducing carbon. Direct carbonate methanation can produce CH₄ given an exogenous supply of H₂ (6–9), as follows:



Here, the production of H₂ is likely to be limited by iron oxidation via water rock reactions, unless conditions are sufficiently reducing that H₂ rather than H₂O is the dominant H-bearing product from magmatic outgassing. In this scenario, however, simultaneously large fluxes and atmospheric concentrations of CO₂ are unlikely (Figure S2).

Hydration of graphite-carbonate bearing rocks can similarly generate CH₄ without the need for iron oxidation (10), in the following reaction:



However, in the absence of biological organic matter, crustal compositions rich in graphite, require strongly reducing conditions (Figure 3). These are unlikely to coexist with high magmatic CO₂ fluxes, which require oxidizing conditions, without large magmatic fluxes of CO (Figure S2).

Some of the other fundamental unknowns with regards to water-rock and metamorphic reactions include the efficiency and extent of hydration reactions under different tectonic regimes, the importance of carbonate hydration in the presence of graphite in generating CH₄, the extent to which H₂ can directly react with carbonates to produce CH₄ under reducing melt conditions, and the extent to which heterogeneous surface environments could simultaneously produce high CH₄ and CO₂ fluxes.

3. Photochemical Destruction and Recombination Pathways for Methane

Methane is removed from an atmosphere photochemically in two ways, depending on the concentration of CO₂ relative to CH₄ and the presence of other oxidants (11). In the first case where CO₂ is more abundant, then CH₄ is destroyed by oxidants and ultimately is converted to CO₂, such as through the following reactions:



or



or



and, subsequently, either

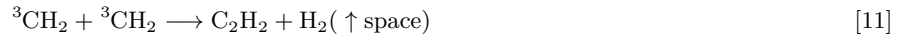


or



The C in H_2CO is further oxidized to CO_2 . The H produced can then be lost to space, thereby irreversibly destroying the CH_4 . Note that OH, O^1D , O and O_2 are byproducts of H_2O and CO_2 photolysis; an atmosphere rich in molecular oxygen is not required for rapid CH_4 destruction (although it does decrease the CH_4 lifetime). The pathway involving OH and O_2 is the dominant destruction pathway in Earth's modern atmosphere, and all of these pathways were likely important for the Archean atmosphere (11).

For the second case where CH_4 is more abundant than CO_2 , CH_4 polymerizes to aerosols, which fall to the ground and remove the atmospheric CH_4 . The chemistry producing aerosols is complex, but this sequence of reactions (Equations 9-14) demonstrates the general process:



These hydrocarbons condense into aerosols that fall to the ground and thus remove CH_4 from the atmosphere. These aerosols could break down and release CH_4 back into the atmosphere or they could get buried and subducted into the planet. However, some portion of the hydrogen produced by methane photolysis will be lost to space, and so, without H_2 replenishment, the C:H ratio of condensate material will rise such that the methane is irreversibly lost.

Ultimately, the lifetime of atmospheric CH_4 is determined by the efficiency of the pathways outlined above. Atmospheric composition is an important determinant of that efficiency. For example, if H_2 is abundant, then CH_4 will efficiently recombine after photolysis via:



where M is an unspecified collision partner that carries away excess energy, which dramatically increases the CH_4 lifetime.

4. Gas Giant Planets

The giant planets in the Solar System contain abundant methane in their H_2 -rich atmospheres due to accreting and processing primordial material from the solar nebula (12, 13). Methane in the atmospheres of giant planets can be replenished indefinitely because, although methane gets photodissociated in the upper atmosphere, hydrogen is never depleted via escape, and carbon and hydrogen can recombine deeper in the atmosphere where temperatures and pressures are high enough for methane production to be thermodynamically favorable and kinetically viable (14). Conversely, temperate terrestrial planets with high mean molecular weight atmospheres and surfaces do not have deep enough atmospheres to replenish methane without an additional source (abiotic or biotic). In terrestrial atmospheres without a replenishment source, methane is photodissociated and hydrogen is lost to space on short timescales (e.g., ~ 10 's of thousands of years for ~ 1 bar atmospheres). However, if a H_2 -rich atmosphere on a terrestrial planet exists, then the CH_4 lifetime would be long due to stabilizing reaction pathways like those that operate in giant planet atmospheres.

5. Super-Earths and Sub-Neptune Planets

Although the focus of this study is on methane biosignatures on terrestrial planets, it is important to consider methane in the atmospheres of super-Earths (planets with radii between 1 and $\sim 1.8 R_{\oplus}$) and sub-Neptunes (radii larger than $\sim 1.8 R_{\oplus}$ and less than $\sim 3.5 R_{\oplus}$) (15). These planets are expected to span a diverse range in bulk compositions from rocky to gaseous, and therefore their atmospheres are also expected to have various compositions, from thick, H_2/He -rich primary atmospheres to thin secondary atmospheres comparable to that of terrestrial planets. Methane in sub-Neptune atmospheres would be unremarkable due to the possibility of thermodynamic recombination at depth. However, future studies could seek to determine the atmospheric pressure necessary for a planet to sustain methane via thermodynamic recombination against photodissociation. Observational methods to distinguish super-Earths from sub-Neptunes are also relevant for excluding deep atmosphere replenishment as a source of methane (16).

When searching for methane in the atmospheres of super-Earths and sub-Neptunes, as is the case for terrestrial planets, it is also important to understand the effects of the host star. For example, M dwarfs tend to be more active longer into their life cycles and have stronger far-UV and weaker near-UV emissions compared to solar-type stars, making it essential to determine how such host stars may impact such an exoplanet's atmosphere (e.g., photochemistry). Future work should aim to couple geochemical and photochemical models to better understand how cooler host stars can affect a planet's atmosphere.

6. Materials and Methods

All codes used in this study are publicly available at <https://github.com/maggiemay13/MethaneBiosignature>.

A. Photochemical Model: PhotochemPy. We use the PhotochemPy photochemical model in Figure S1 to illustrate the methane fluxes required to sustain atmospheric methane in various atmospheres. PhotochemPy is a descendant of the Photochem model contained in the Atmos modeling suite, which was originally developed by Jim Kasting and Kevin Zahnle (17) and has since been developed by many of their students and colleagues. Appendix B in (18) contains an in-depth description of the main equations solved in the Photochem model. The physics and chemistry in PhotochemPy are very similar to the physics and chemistry in the version of Atmos used in (2). The main exception is that we have updated several reactions, and water photolysis cross sections following (19). However, PhotochemPy deserves a distinct name because it is a modern Fortran rewrite of the original Fortran 77 code. Additionally, PhotochemPy uses Numpy F2PY (20) to generate a Python wrapper to the compiled Fortran library ((3), <https://github.com/Nicholaswogan/PhotochemPy>).

B. Carbon Partitioning and Magmatic Outgassing Calculations. For Figure 3 and Figure S2, to calculate how carbon partitions between different phases under various redox conditions for ~ 10 km of crust (pressures from ~ 0.5 GPa and solidus temperatures from ~ 1400 - 1445 K), we follow the melting and volatile partitioning methods outlined in (21). We first compute batch melting with standard partition coefficients for CO_2 and H_2O which returns how concentrated CO_2 and H_2O are in the melt for a given melt fraction, F :

$$X_{CO_2}^{\text{melt}} = (1 - (1 - F))^{1/0.002} (m_{\text{mantle}, CO_2} / m_{\text{mantle}}) / F \quad [16]$$

$$X_{H_2O}^{\text{melt}} = (1 - (1 - F))^{1/0.01} (m_{\text{mantle}, H_2O} / m_{\text{mantle}}) / F \quad [17]$$

where m_{mantle} is the mantle mass (in kg, which for Earth is 4×10^{24} kg) and m_{mantle, CO_2} and m_{mantle, H_2O} are the masses of CO_2 and H_2O in the mantle, respectively (in kg). However, if the source material is reducing, the melt will never get this carbon rich due to graphite saturation. Therefore, we compute the carbon melt concentration assuming graphite saturation. We assume the carbon is stored in the mantle as graphite and dissolves into the melt as carbonate ions (CO_3^{2-}). The amount of carbonates dissolved in the melt are calculated from equilibrium constants K_1 and K_2 :

$$X_{CO_3^{2-}}^{\text{melt}} = \frac{K_1 K_2 f_{O_2}}{1 + K_1 K_2 f_{O_2}} \quad [18]$$

$$\log_{10} K_1 = 40.07639 - 2.53932 \times 10^{-2} T + 5.27096 \times 10^{-6} T^2 + 0.0267 \frac{(P - 1)}{T} \quad [19]$$

$$\log_{10} K_2 = -6.24763 - \frac{282.56}{T} - 0.119242 \frac{(P - 1000)}{T} \quad [20]$$

for temperature (T , in K) and pressure (P , in bars) and f_{O_2} , which is the oxygen fugacity calculated based on the Iron-Wüstite redox buffer:

$$f_{O_2} = 10^{-27215/T + 6.57 + 0.0552(P-1)/T} \quad [21]$$

Then, we calculate the CO_2 melt abundance:

$$X_{CO_2}^{\text{melt}} = \left[\frac{M_{CO_2}}{f_{wm}} X_{CO_3^{2-}}^{\text{melt}} \right] / \left[1 - \left(1 - \frac{M_{CO_2}}{f_{wm}} \right) X_{CO_3^{2-}}^{\text{melt}} \right] \quad [22]$$

where M_{CO_2} is CO_2 's molar mass and f_{wm} is the formula weight of the melt (36.594) (21). We take the minimum of the graphite-saturated CO_2 melt concentration (Equation 22) and the constant partition coefficient concentration (Equation 16) and use that $X_{CO_2}^{melt}$ value to calculate the flux of CO_2 in the melt:

$$F_{CO_2}^{melt} = X_{CO_2}^{melt} m_{melt} F \quad [23]$$

where m_{melt} is the planetary melt production rate (in g/s, where Earth's nominal melt production rate is 3.2×10^9 g/s). To compare the original carbon content to the amount that remains as graphite, we compute:

$$\text{Original Carbon} = \frac{m_{\text{mantle}, CO_2}}{m_{\text{mantle}}} m_{melt} \quad [24]$$

$$\text{Remaining Graphite} = \text{Original Carbon} - F_{CO_2}^{melt} \quad [25]$$

For the Monte Carlo simulation, we vary the input parameters and sample distributions according to Table S1.

To calculate the species that would be released by magmatic outgassing and their corresponding outgassing fluxes, we use the outgassing speciation model described in (22). As magma ascends to the surface, the overburden pressure decreases and the dissolved volatiles in the magma may reach saturation. At that point, volatiles exsolve from the magma and form gas bubbles, which can be released to the atmosphere. In addition, chemical reactions take place within the bubbles which can alter their chemical compositions. This model estimates the composition of these gas bubbles just prior to their release to the atmosphere by solving a system of equations including the Iacono-Marziano solubility relationships for H_2O and CO_2 , gas-phase equilibrium relationships and mass conservation of hydrogen and carbon (22). The model assumes that the oxygen fugacity of the gas is set by the oxygen fugacity of the magma and requires the following inputs: initial concentrations of H_2O and CO_2 in the melt prior to outgassing, temperature and pressure of outgassing, and redox state of the melt. Please refer to (22) for further details.

Swain et al. 2021 (23) recently claimed the detection of a thin, reducing atmosphere around the rocky exoplanet GJ 1132 b that is H_2 -dominated and rich in CH_4 ($\sim 0.5\%$). They simulated mantle outgassing and argued that an ultra-reduced magma could reproduce the observed atmosphere, with the best fitting model parameters giving an extremely reduced oxygen fugacity of $\log f_{O_2} = IW - 11$ (23). Such reduced conditions could conceivably arise if significant amounts of hydrogen from a planet's primary atmosphere dissolve into the magma ocean and were sequestered into the interior, thereby providing a reservoir of volatiles that can later be outgassed to form a secondary atmosphere (23, 24). However, the outgassing model of (23) omits carbon partitioning between solid, liquid and gas phases under ultra-reducing redox conditions.

We find that for an ultra-reduced melt of $\log f_{O_2} = IW - 11$, essentially all of the carbon ($>99\%$) will remain saturated as graphite during partial melting, so there is negligible carbon available for gaseous phases (Figure 3). To confirm this, we used the above outgassing speciation model which solves for the gas-gas and gas-melt equilibrium in a C-O-H system, to predict the gases that would be released from the melt by magmatic outgassing. From this model, we determine that the CH_4 , CO_2 , and CO outgassing fluxes would be negligible ($<1E-10$ Tmol/year) at such a reduced oxygen fugacity (Figure S2). It is important to note that these calculations do not include carbon in the form of iron carbonyls and methyl (CH_3) groups bonded to Si^{4+} in the melt as some studies have suggested will be present under reducing conditions (25, 26). However, it is not expected that these additional carbon-bearing species will significantly alter our findings as these studies also found carbon stable in the melt under reducing conditions. Therefore our findings suggest that the outgassing mechanism proposed for GJ 1132 b is improbable. Additionally, an independent study that analyzed the same Hubble Space Telescope (HST) transit data found no methane signature and instead claim a featureless spectrum for GJ 1132 b (27), and the findings of (23) conflict with Lyman-alpha observations of the system (28).

C. Calculations of Global CH_4 Flux Estimates from Abiotic Sources. The global CH_4 flux estimates for different abiotic sources in Table S2 (and illustrated in the schematic Figure 2) and Figure 4 are calculated as follows:

Higher Temperature:

- **Etioppe & Lollar 2013:** To determine an estimated global abiotic CH_4 flux from surface volcanism, we take their CH_4 flux estimates for individual volcanoes and multiply these values by the number of active volcanoes on Earth today (~ 1500) (6).
- **Ryan et al. 2006:** To determine an estimated global abiotic CH_4 flux from surface volcanism, we followed the same procedure as described above for Etioppe & Lollar 2013, except with Ryan et al.'s estimates for individual volcanic outgassing CH_4 fluxes (29).
- **Schindler & Kasting 2000:** They estimated the current global CH_4 flux from submarine volcanism to be $\sim 10^{-2}$ Tmol/year by taking an observed ratio of CH_4/CO_2 in mid-ocean ridge hydrothermal vent fluids and an estimated total outgassed carbon flux at the mid-ocean ridges.

Lower Temperature:

Observational and Theoretical Studies:

- **Cannat et al. 2010:** They derive a global serpentinization-related methane flux at slow spreading mid-ocean ridges of 2.5×10^{-2} Tmol/year (30).

- **Keir 2010:** Keir calculates a global methane flux of 2×10^{-2} Tmol/year from mid-ocean ridges, similar to the findings of Cannat et al. 2010 (31).
- **Jones et al. 2010:** Their serpentinization experiments for mid-ocean ridges and forearcs determined CH_4 production rates ranging from 1×10^{-5} to $0.05 \mu\text{mol/kg/hr}$ (32). Taking these rates and extrapolating to the mass of the entire oceanic crust, we find that the corresponding global abiotic CH_4 estimates exceed the Earth's iron supply. However McCollom 2013 (33) caution that Jones et al. did not determine their background levels of CH_4 so it is possible that a portion of the methane generated in their experiments came from sources of contamination. Therefore, the findings of Jones et al. cannot be extrapolated to a global abiotic flux.
- **Catling & Kasting 2017:** Using a combination of different observational studies, they determined abiotic CH_4 flux estimates for hot, axial vents and off-axis vent fields of 0.015 and 0.03 Tmol/year, respectively (4). For hot, axial vents, they estimated the abiotic CH_4 flux by using observed CH_4 and CO_2 concentrations from East Pacific Rise fluids. For the off-axis vent fields, they used an estimated H_2 flux and the CH_4/H_2 ratio in ultramafic vent fields to determine an abiotic CH_4 flux estimate (4).
- **Guzmán-Marmolejo et al. 2013:** They estimated the amount of CH_4 generated by serpentinization in hydrothermal vent systems. For $1M_{\oplus}$ and $5M_{\oplus}$ planets, they determined abiotic CH_4 fluxes of 0.18 Tmol/year and 0.35 Tmol/year, respectively (34). These estimates account for the supply rate of available FeO in the crust which is determined in part by the crustal production rate. For the $5M_{\oplus}$ planet, the crustal production rate is scaled from Earth using a power law. They also take into account the limitations of CO_2 in hydrothermal systems based on different observational studies.
- **Kasting 2005:** Kasting 2005 estimated the global abiotic CH_4 flux from off-axis mid-ocean ridges by extrapolating from observed methane concentrations in hydrothermal fluids. They found that, at present, the abiotic hydrothermal CH_4 flux is ~ 0.1 Tmol/year, but during the Hadean the flux may have been larger, ~ 1.5 Tmol/year (35). They note that if seafloor creation during the Hadean was much faster, the abiotic CH_4 flux could have increased by a factor of 5-10. However, given that seafloor production rates during that period are uncertain, we only include their Hadean estimate of 1.5 Tmol/year in Figure 4 and Table S2. These estimates are about an order of magnitude larger than those of Catling & Kasting 2017 because Kasting 2005 assumed a larger water circulation rate compared to that of Catling & Kasting 2017 (4). In addition, the Kasting 2005 Hadean abiotic flux estimate is larger than Guzman-Marmolejo et al.'s estimates because Guzman-Marmolejo took into account the iron supply and CO_2 limitations in hydrothermal systems (34, 35).
- **Brovarone et al. 2017:** This study determined several different global CH_4 flux estimates for different sites where serpentinization takes place including subduction zone fluids, forearc mantle wedges above subduction zones, and sub-seafloor conditions (36).
- **Fiebig et al. 2007:** They investigated subduction-related hydrothermal sites in the Mediterranean and computed both an uppermost flux estimate for abiogenic CH_4 during the Archean (2.5-5 Tmol/year) and a present-day flux (6×10^{-3} Tmol/year) (37).
- **Fiebig et al. 2009:** This study estimated the abiogenic CH_4 flux from continental hydrothermal systems to be 0.31 Tmol/year (38).
- **Portella et al. 2019:** Their study of serpentinization of chromitites in ophiolites found that chromitites can contain CH_4 gas concentrations up to $0.31 \mu\text{g/g}_{\text{rock}}$. Taking this CH_4 concentration and multiplying it by Earth's melt production rate (3.2×10^9 g/s) results in a global CH_4 flux estimate of 2×10^{-3} Tmol/year (39).
- **Klein et al. 2019:** They studied methane formation in olivine-hosted secondary fluid inclusions to inform serpentinization in subduction zones, mid-ocean ridges and ophiolites. They determined that the Chimaera serpentinization system has released 0.076 to 0.5 km^3 CH_4 during the past 2000 years which is equivalent to 2×10^6 - 11×10^6 mol/year of CH_4 . They also estimated that the lower oceanic crust contains a total of ~ 300 Tmol of CH_4 gas (40). Given that the lifetime of the oceanic crust is ~ 200 Myrs, the estimated global abiotic CH_4 flux due to serpentinization is 1.5×10^{-6} Tmol/year.

Experiments:

- **McCollom 2013:** The hydrocarbon formation experiments discussed in McCollom 2013 measure the amount of dissolved CH_4 gas in serpentinized olivine at 300°C as a function of time (see their Figure 7). Taking their experimental methane production rate of $0.05 \mu\text{mol/kg/hr}$ and scaling it to the entire mass of oceanic crust on Earth ($\sim 6 \times 10^{21}$ kg) results in a global flux estimate that exceeds Earth's iron supply (33). Such an estimate requires the whole crust to be at a high temperature which is unrealistic for a habitable zone terrestrial planet. Therefore, it is not possible to extrapolate their experimental findings to a global abiotic flux rate.
- **Oze et al. 2012:** They performed experiments to investigate the influence of mineral catalysts on serpentinization and found that the CH_4 production rate varied from ~ 0.09 to $0.15 \mu\text{mol/kg/hr}$. If we take their experimental CH_4 production rates and extrapolate to the mass of the oceanic crust, we find a global CH_4 flux estimate that exceeds Earth's iron supply. As with Jones et al. (32), McCollom 2013 (33) note that Oze et al. did not quantify their background levels of CH_4 , so it is not possible to properly extrapolate a global abiotic CH_4 flux from their experiments.

- **Neubeck et al. 2011:** Their serpentinization experiments on forsteritic olivine determined CH₄ accumulation rates ranging from 2.7×10^{-11} to 7.3×10^{-11} mol/m²/s. However, McCollom 2013 (33) noted that Neubeck et al. did not quantify their background CH₄ levels, so it is not possible to extract an abiotic global flux estimate from this study.
- **McCollom 2016:** They performed serpentinization experiments with olivine and measured a range of dissolved CH₄ concentrations from 5.5 to 270 μmol/kg_{olivine}. They used isotopic labeling to differentiate CH₄ produced by serpentinization from background sources, and found that in almost all experiments, the majority of CH₄ produced actually derived from background sources rather than from reduction of dissolved inorganic carbon. Using the isotopic labeling, for the experiments performed at or above 300 °C, the amount of CH₄ generated via reduction of inorganic carbon was 16-50 μmol/kg_{olivine} (41). Taking these concentrations, dividing by the duration of the experiments and extrapolating to the mass of the oceanic crust, we find that the corresponding global abiotic CH₄ estimates exceed the Earth's iron supply. As with McCollom 2013, these experiments suggest that high temperatures are necessary to generate CH₄. Such temperatures are higher than typical temperatures for habitable zone terrestrial planets. Therefore, we cannot properly extrapolate these experimental findings to a global abiotic CH₄ flux on temperate terrestrial planets.

Impacts:

- **Kasting 2005:** Kasting estimated the global CH₄ flux due to impact events during the Hadean to be 1.24 Tmol/year (35).
- **Kress & McKay 2004:** They determined that 0.6 Tmol of CH₄ is generated by a 1-km cometary impactor (42).
- **Zahnle et al. 2020:** For a highly-reduced Pluto-sized dwarf planet impactor, they determined that it would generate ~2300 moles CH₄/cm² (11).
- **Court & Sephton 2009:** Experimentally studied ablation of carbonaceous chondritic materials and found that they release <100 ppm of CH₄ at temperatures up to 1000°C (43).

D. Calculations of Atmospheric Methane Lifetime for Volatile-Rich Bodies. In Figure 5, we estimate the atmospheric lifetime of methane for an Earth-mass terrestrial planet with different water mass fractions and Titan-like initial volatile inventories. Using model calculations based on Cassini data for Titan's interior composition from (44), we assume Titan's volatile content consists of 0.35 % CH₄ and ~4-6 % CO₂ relative to weight % H₂O (44). We conservatively assume that the escape flux of hydrogen is diffusion-limited and calculate the atmospheric lifetime of CH₄. First we calculate the mass of methane:

$$m_{CH_4} = (0.35/100)m_{H_2O} \quad [26]$$

where m_{H_2O} is the water mass fraction of the planet (in kg). Then we calculate the diffusion-limited escape flux of H₂.

$$\Phi = C f_T(H_2) \quad [27]$$

Φ is the escape flux of H₂ from Earth at the diffusion limit (in molecules/cm²/s). Assuming the atmosphere is 10% CH₄, the fraction of hydrogen ($f_T(H_2)$) is 0.2 (i.e., $0.1 \times 2 = 0.2$ with two H₂ molecules per CH₄ molecule) and C for Earth's atmosphere is 2.5×10^{13} cm⁻²s⁻¹. The atmospheric lifetime of CH₄ (in years) is given by:

$$T_{CH_4} = \left(\frac{m_{CH_4}}{M_{CH_4}} NA \right) / (\Phi \times SA \times 3.154 \times 10^7) \quad [28]$$

where M_{CH_4} is the molar mass of CH₄ in mol/kg, NA is the Avogadro constant and SA is the surface area of the Earth (in cm²). Table S3 demonstrates how the lifetime of atmospheric CH₄ increases with increasing planetary mass fraction of water. For Figure 5, we ran a Monte Carlo simulation and varied the CH₄ inventory, sampling a uniform distribution from 10⁻⁴ to 10⁻² relative to weight % water, for water mass fractions from 10⁻² to 10 weight % of the planet's mass (assuming an Earth-mass planet).

To check that our estimated CH₄ atmospheric mixing ratio of 10% is reasonable, we calculate the solubilities of CH₄ and CO₂ for the atmosphere-ocean system reservoir using Henry's Law partitioning. For CH₄:

$$(C \times m_{H_2O} \times M_{CH_4}) + m_{atm} = m_{CH_4} \quad [29]$$

where m_{H_2O} and m_{CH_4} are the masses of H₂O and CH₄, respectively. M_{CH_4} is CH₄'s molar mass (kg/mol) and m_{atm} is the mass of the atmosphere, given by:

$$m_{atm} = PA/g \quad [30]$$

where P is pressure in bars, A is the surface area of the planet in m², and g is surface gravity (9.8 m/s²). $[CH_4]$ is the concentration of dissolved CH₄ (mol/kg), which is given by Henry's Law:

$$[CH_4] = kP \quad [31]$$

where k is Henry's Law constant (0.0014 mol/kg/bar for CH₄). Solving for pressure, we find that for an Earth-mass planet with 1% of its mass consisting of water, the pressure of methane is ~32 bars. Following the same formalism above for CO₂, which has a Henry's Law constant of 0.04 mol/kg/bar, its pressure is ~22 bars. Therefore, our choice of CH₄'s atmospheric mixing ratio of 10% is conservative given the volatile inventories, which also allow for plausible inventories of N₂ gas.

We also consider whether volatile-rich, habitable zone planets could produce a long-lived CH₄+CO₂ biosignature false positive if not all water is melted. The storage and slow release of CH₄ and CO₂ from clathrates (ices that trap gases) on a Titan-like planet could conceivably mimic a biosphere. If surface conditions are habitable, however, then storage of large volumes of CH₄ in pure clathrates is not possible because CH₄ clathrates are less dense than liquid water at all pressures (45). Any CH₄ clathrates stored in high pressure ices would therefore rise to the surface and rapidly dissociate. It is true that methane clathrates are a CH₄ reservoir on Earth, but this is only because they are trapped by the weight of sediments above them, and are thus in a quasi-stable state (and will be potentially perturbed by slight surface warming). The weight of sediments could not trap the ~10²² mol of CH₄ required to sustain biogenic-like fluxes of CH₄ for Gyr timescales.

If surface conditions are sub-freezing, CH₄ clathrates can inhibit subsurface ocean formation at all depths, and tectonically driven ice resurfacing may continuously bring fresh clathrates to the surface, maintaining CH₄ fluxes larger than Earth's biological flux (46). The region of parameter space for which atmospheric CH₄ can be maintained is likely small, however, since clathrates are unstable against surface warming: liquid water from warming will destabilize CH₄ clathrates, causing CH₄ release into the atmosphere and even more greenhouse warming (46). Initial surface temperatures must therefore be low to prevent this runaway melting. For many planets, clathrate false positives may be ruled out by estimating minimum surface temperatures from observed atmospheric gases and plausible albedos. However, additional modeling work is required to characterize clathrate-atmosphere interactions across diverse planetary conditions.

Input Parameter	Low	High	Sampling Method
Mantle Mass (M_{mantle}) (kg)	0.1(4×10^{24})	10(4×10^{24})	\log_{10} Uniform Distribution
Mantle CO ₂ Mass ($M_{\text{mantle, CO}_2}$) (kg)	1×10^{-5} (4×10^{24})	1×10^{-2} (4×10^{24})	\log_{10} Uniform Distribution
Mantle H ₂ O Mass ($M_{\text{mantle, H}_2\text{O}}$) (kg)	1×10^{-5} (4×10^{24})	1×10^{-1} (4×10^{24})	\log_{10} Uniform Distribution
Melt Fraction (F)	0.1	0.5	Uniform Distribution
Planetary Melt Production (M_{melt}) (g/s)	0.1(3.2×10^9)	10(3.2×10^9)	\log_{10} Uniform Distribution

Table S1. Monte Carlo sampling distributions for carbon partitioning and gas speciation calculations.

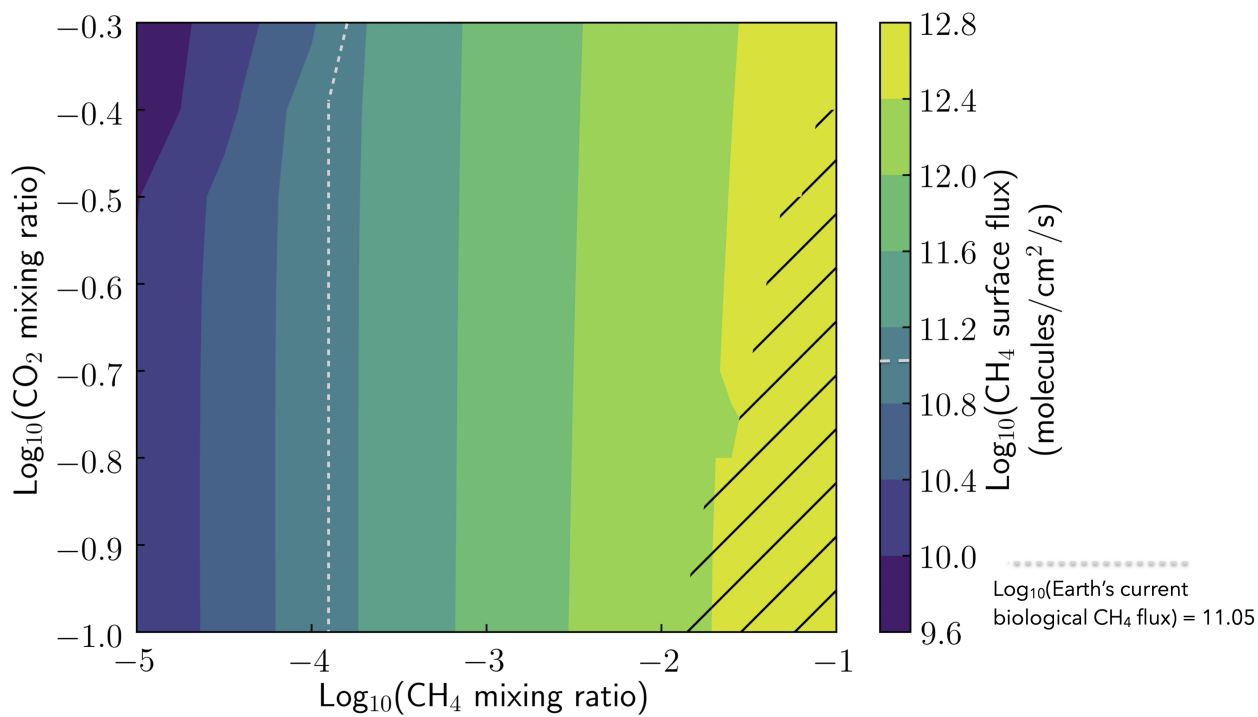


Fig. S1. Methane surface flux required to sustain CH₄- and CO₂-rich atmospheres in photochemical steady state. Using PhotochemPy, we ran a series of models with an initial atmospheric composition that is Archean Earth-like (orbiting the Sun at 2.7 Ga) exploring a range of CH₄ and CO₂ surface mixing ratios from 10⁻⁵ to 0.1 and 0.1 to 0.5, respectively. The contour colors correspond to the CH₄ surface flux required to sustain the atmospheric mixing ratios. While the model accounts for haze formation, we found that at higher CH₄ mixing ratios, the model had trouble converging to a steady-state solution. For those cases corresponding to the hatched region of the figure, we ran models that used the same Archean Earth-like initial atmospheric composition but removed the haze component in order to ensure model convergence. Ultimately, for abundant atmospheric CH₄ (i.e., surface mixing ratios above ~10⁻³) to be stable against photochemistry in terrestrial planet atmospheres requires a significant replenishment source that results in large CH₄ surface fluxes that are likely much larger than Earth's current biological flux.

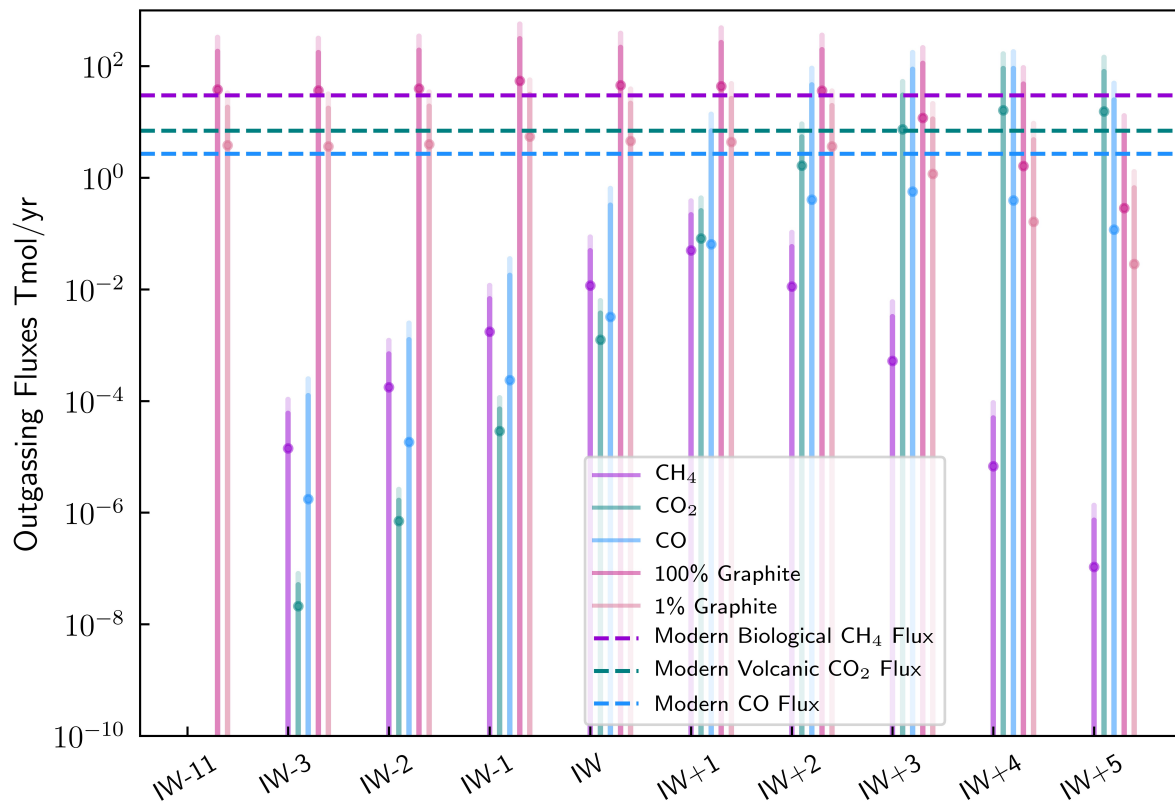


Fig. S2. Simultaneous outgassing of CH₄ and CO₂ with negligible CO is highly unlikely unless large quantities of graphite are efficiently converted to CH₄ via metamorphism. Outgassing fluxes as a function of oxygen fugacity. We used the same batch-melting model as described in Figure 3 and solved for speciation of gases produced by magmatic outgassing. The results are the average outgassing fluxes (in Tmol/year) of CH₄, CO₂ and CO from the Monte Carlo simulation with uncertainties reported as the 95% confidence intervals. The graphite results assume that either 100% or 1% of the remaining graphite can be converted into outgassed CH₄. The horizontal dashed lines show current outgassing fluxes on Earth for reference (e.g., biological CH₄ flux). For a planet with a very reduced melt composition, outgassing of any carbon species (i.e., CH₄, CO₂, and CO) will be negligible. In addition, for all oxygen fugacities considered from extremely reduced ($IW - 11$) to highly oxidized ($IW + 5$), the magmatic outgassing fluxes of CH₄ are still orders of magnitude lower than Earth's modern biological CH₄ flux of 30 Tmol/year.

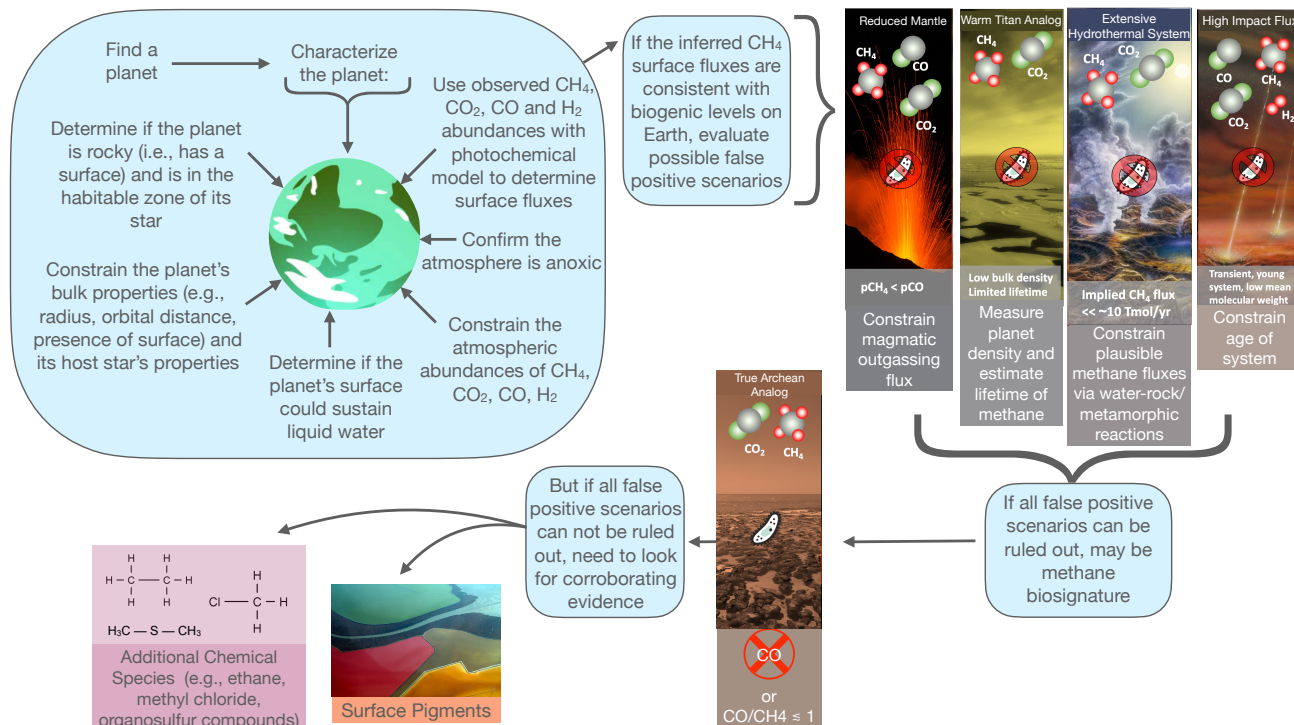


Fig. S3. Possible procedure to search for methane biosignatures on terrestrial exoplanets that takes into account the planetary context. Once an exoplanet has been detected, it is important to characterize its bulk properties (e.g., mass, radius, orbital properties, presence of a surface, host star properties). In addition, constraining its atmospheric composition, particularly the abundances CH_4 , CO_2 , CO , H_2 , H_2O and confirming that the atmosphere is anoxic, is essential for determining the presence of a methanogenic biosphere. Using this data with a photochemical model can determine the surface fluxes of the different atmospheric constituents that are necessary to sustain the observed atmospheric abundances. If the inferred CH_4 surface fluxes are consistent with plausible biogenic levels, then all possible false positive scenarios must be evaluated. If all false positives can be definitively ruled out then a methane biosignature has been identified at a high level of confidence that must be statistically determined. However, if all false positives cannot be ruled out, then it is necessary to look for corroborating evidence like additional gas species (e.g., methyl chloride, and organosulfur compounds) and the presence of surface pigments. Credits (images): Don Dixon, Wikimedia Commons; Donald Hobern; kuhnmi; NASA/JPL-Caltech/Lizbeth B. De La Torre; Doc Searls.

Abiotic Source	Reference	CH ₄ Flux	Global CH ₄ Flux Estimate
Higher Temperature			
Volcanic	Etioppe & Lollar 2013 (6)	100 tons/yr (Mt. Etna, most Icelandic volcanoes)	9.4E-3 Tmol/year
Submarine Volcanism	Ryan et al. 2006 (29) (47)	9 tons/yr	8.4E-4 Tmol/yr 1.3E-2 Tmol/year
Lower Temperature			
Serpentinization at slow-spreading mid-ocean ridges	Cannat et al. 2010 (30)	3.9E7 mol/yr (Rainbow Hydrothermal Field); 0.04-0.3E7 mol/km/yr (Ridge domains with frequent ultra-mafic outcrops)	2.5E-2 Tmol/yr
Serpentinization in vent fluids from mid-ocean ridges	Keir 2010 (31)	0.1-4 mmol/kg	2E-2 Tmol/yr
Serpentinization at seafloor hydrothermal systems	Calling & Kasting 2017 (4)	–	0.015 - 0.03 Tmol/year
Serpentinization at hydrothermal vent systems	Guzmán-Marmolejo et al. 2013 (34)	–	0.18 Tmol/year (for 1 M _{Earth}), 0.35 Tmol/year (for 5 M _{Earth})
Serpentinization at off-axis mid-ocean ridges	Kasting 2005 (35)	–	0.1 Tmol/year (at present), 1.5 Tmol/year (during Hadean)
Serpentinization and carbonate reduction at subduction zones	Brovarone et al. 2017 (36)	–	9E-2 Tmol/yr (subduction zone fluids); 8E-3-0.2 Tmol/yr (forearc mantle wedges above subduction zones); 1E-2-0.1 Tmol/yr (sub-seafloor)
Serpentinization at subduction-related sites (and estimates for Archean Eon)	Fiebig et al. 2007 (37)	–	2.5-5 Tmol/yr (during Archean), 6E-3 Tmol/yr (at present)
Reduction of CO ₂ in continental hydrothermal systems	Fiebig et al. 2009 (38)	–	0.31 Tmol/year
Serpentinization of chromitites in ophiolites	Portella et al. 2019 (39)	0.31 μg/g (rock) in chromitites	2E-3 Tmol/yr
Serpentinization in subduction zones, mid-ocean ridges and ophiolites	Klein et al. 2019 (40)	2E6-11E6 mol/yr (Chimaera system)	1.5E-6 Tmol/yr
Experiments of hydrocarbon formation in deep subsurface	McCollon 2013 (33)	0.05 μmol/kg/hr	CH ₄ Flux > Fe supply
Serpentinization experiments for mid-ocean ridges and forearcs	Jones et al. 2010 (32)	1E-5 - 0.06 μmol/kg/hr	CH ₄ Flux > Fe supply*
Serpentinization experiments investigating mineral catalysts	Oze et al. 2012 (48)	0.15 μmol/kg/hr	CH ₄ Flux > Fe supply*
Serpentinization experiments on forsteritic olivine	Neubeck et al. 2011 (49)	2.7E-11-7.3E-11 mol/m ² /s	0.64-1.2 Tmol/yr*
Serpentinization experiments on olivine	McCollon 2016 (41)	~7.7E-3-1.3E-2 μmol/kg _{olivine} /hr	CH ₄ Flux > Fe supply
Impacts			
Impact events during the Hadean	Kasting 2005 (35)	–	1.24 Tmol/year
Cometary impact events	Kress & McKay 2004 (42)	0.6 Tmol (generated by 1-km comet impactor)	–
Impact events for early Earth	Zahnle et al. 2020 (11)	2300 moles/cm ² (generated by a highly-reduced Pluto-sized dwarf planet impactor)	Not applicable - transient event lasting ~10,000 years
Meteorite ablation experiments	Court & Sephton 2009 (43)	<100 ppm from gasification of carbonaceous asteroid	–

Table S2. Summary of abiotic CH₄ sources and their estimated global CH₄ flux values. *Indicates that the experimental measurements may have over-estimated the amount of methane generated due to the presence of background sources.

Mass Fraction of Water (wt% of planet mass)	0.1	1.0	10	50
Lifetime of CH ₄ (Myr)	1	10	100	500

Table S3. Estimated lifetime of atmospheric CH₄ for Earth-mass terrestrial planets with Titan-like initial volatile inventory and different size water mass fractions.

References

1. P Woitke, et al., Coexistence of ch₄, co₂, and h₂o in exoplanet atmospheres. *Astron. Astrophys.* **646**, 10 (2021).
2. G Arney, et al., The pale orange dot: The spectrum and habitability of hazy archean earth. *Astrobiology* **16**, 873–899 (2016).
3. N Wogan, Photochempy v0.1.0. *Zenodo* <https://doi.org/10.5281/zenodo.6360737> (2022).
4. DC Catling, JF Kasting, *Atmospheric Evolution on Inhabited and Lifeless Worlds*. (Cambridge University Press), (2017).
5. J Krissansen-Totton, S Olson, DC Catling, Disequilibrium biosignatures over earth history and implications for detecting exoplanet life. *Sci. Adv.* **4**, 14 (2018).
6. G Etiope, BS Lollar, Abiotic methane on earth. *Rev. Geophys.* **51**, 276–299 (2013).
7. AA Giardini, CA Salotti, JF Lakner, Synthesis of graphite and hydrocarbons by reaction between calcite and hydrogen. *Science* **159**, 317–319 (1968).
8. A Reller, C Padeste, P Hug, Formation of organic carbon compounds from metal carbonates. *Nature* **329**, 527–529 (1987).
9. N Yoshida, T Hattori, E Komai, T Wada, Methane formation by metal-catalyzed hydrogenation of solid calcium carbonate. *Catal. Lett.* **58**, 119–122 (1999).
10. JR Holloway, Graphite-ch₄-h₂o-co₂ equilibria at low-grade metamorphic conditions. *Geology* **12**, 455–458 (1984).
11. KJ Zahnle, R Lupu, DC Catling, N Wogan, Creation and evolution of impact-generated reduced atmospheres of early earth. *The Planet. Sci. J.* **1**, 11 (2020).
12. MH Wong, PR Mahaffy, SK Atreya, HB Niemann, TC Owen, Updated galileo probe mass spectrometer measurements of carbon, oxygen, nitrogen, and sulfur on jupiter. *Icarus* **171**, 153–170 (2004).
13. LN Fletcher, GS Orton, NA Teanby, PGJ Irwin, GL Bjoraker, Methane and its isotopologues on saturn from cassini/cirs observations. *Icarus* **199**, 351–367 (2009).
14. JI Moses, et al., Photochemistry and diffusion in jupiter’s stratosphere: Constraints from iso observations and comparison with other giant planets. *J. Geophys. Res.* **110**, 45 (2005).
15. BJ Fulton, et al., The california-kepler survey. iii. a gap in the radius distribution of small planets. *The Astron. J.* **154**, 109 (2017).
16. X Yu, JI Moses, JJ Fortney, X Zhang, How to identify exoplanet surfaces using atmospheric trace species in hydrogen-dominated atmospheres. *The Astrophys. J.* **914**, 18 (2021).
17. JF Kasting, KJ Zahnle, JCG Walker, Photochemistry of methane in the earth’s early atmosphere. *Precambrian Res.* **20**, 121–148 (1983).
18. DC Catling, JF Kasting, *Atmospheric Evolution on Inhabited and Lifeless Worlds*. (Cambridge University Press), (2017).
19. S Ranjan, et al., Photochemistry of anoxic abiotic habitable planet atmospheres: Impact of new h₂o cross sections. *The Astrophys. J.* **896**, 21 (2020).
20. P Peterson, F2py: a tool for connecting fortran and python programs. *Int. J. Comput. Sci. Eng.* **4** (2009).
21. G Ortenzi, et al., Mantle redox state drives outgassing chemistry and atmospheric composition of rocky planets. *Sci. Reports* **10**, 14 (2020).
22. N Wogan, J Krissansen-Totton, DC Catling, Abundant atmospheric methane from volcanism on terrestrial planets is unlikely and strengthens the case for methane as a biosignature. *The Planet. Sci. J.* **1**, 58 (2020).
23. MR Swain, et al., Detection of an atmosphere on a rocky exoplanet. *The Astron. J.* **161**, 213 (2021).
24. ES Kite, BF Jr., L Schaefer, EB Ford, Superabundance of exoplanet sub-neptunes explained by fugacity crisis. *The Astrophys. J.* **887**, L33 (2019).
25. DT Wetzell, MJ Rutherford, SD Jacobsen, EH Hauri, AE Saal, Degassing of reduced carbon from planetary basalts. *Proc. Natl. Acad. Sci.* **110**, 8010–8013 (2013).
26. BO Mysen, K Kumamoto, GD Cody, ML Fogel, Solubility and solution mechanisms of c-o-h volatiles in silicate melt with variable redox conditions and melt composition at upper mantle temperatures and pressures. *Geochimica et Cosmochimica Acta* **75**, 6183–6199 (2011).
27. LV Mugnai, et al., Ares. v. no evidence for molecular absorption in the hst wfc3 spectrum of gj 1132 b. *The Astron. J.* **161**, 284 (2021).
28. WC Waalkes, et al., Ly in the gj 1132 system: Stellar emission and planetary atmospheric evolution. *The Astron. J.* **158** (2019).
29. S Ryan, EJ Dlugokencky, PP Tans, ME Trudeau, Mauna loa volcano is not a methane source: Implications for mars. *Geophys. Res. Lett.* **33**, L12301 (2006).
30. M Cannat, F Fontaine, J Escartin, Serpentinization and associated hydrogen and methane fluxes at slow spreading ridges in *Diversity of Hydrothermal Systems on Slow Spreading Ocean Ridges*, eds. PA Rona, CW Devey, J Dymont, BJ Murton. (American Geophysical Union) Vol. 188, pp. 241–264 (2010).
31. RS Keir, A note on the fluxes of abiogenic methane and hydrogen from mid-ocean ridges. *Geophys. Res. Lett.* **37**, L24609 (2010).
32. CL Jones, R Rosenbauer, JI Goldsmith, C Oze, Carbonate control of h₂ and ch₄ production in serpentinization systems at elevated p-ts. *Geophys. Res. Lett.* **37**, L14306 (2010).
33. TM McCollom, Laboratory simulations of abiotic hydrocarbon formation in earth’s deep subsurface. *Rev. Mineral. Geochem.* **75**, 467–494 (2013).
34. A Guzmán-Marmolejo, A Segura, E Escobar-Briones, Abiotic production of methane in terrestrial planets. *Astrobiology*

- 13, 550–559 (2013).
35. JF Kasting, Methane and climate during the precambrian era. *Precambrian Res.* **137**, 119–129 (2005).
 36. AV Brovarone, et al., Massive production of abiogenic methane during subduction evidenced in metamorphosed ophicarbonates from the italian alps. *Nat. Commun.* **8**, 13 (2017).
 37. J Fiebig, AB Woodland, J Spangenberg, W Oschmann, Natural evidence for rapid abiogenic hydrothermal generation of ch₄. *Geochimica et Cosmochimica Acta* **71**, 3028–3039 (2007).
 38. J Fiebig, AB Woodland, W D'Alessandro, W Püttmann, Excess methane in continental hydrothermal emissions is abiogenic. *Geology* **37**, 495–498 (2009).
 39. Y de Melo Portella, F Zaccarini, G Etiope, First detection of methane within chromitites of an archean-paleoproterozoic greenstone belt in brazil. *Minerals* **9**, 15 (2019).
 40. F Klein, NG Grozeva, JS Seewald, Abiotic methane synthesis and serpentinization in olivine-hosted fluid inclusions. *Proc. Natl. Acad. Sci.* **116**, 17666–17672 (2019).
 41. TM McCollom, Abiotic methane formation during experimental serpentinization of olivine. *Proc. Natl. Acad. Sci.* **113**, 13965–13970 (2016).
 42. ME Kress, CP McKay, Formation of methane in comet impacts: implications for earth, mars, and titan. *Icarus* **168**, 475–483 (2004).
 43. RW Court, MA Sephton, Meteorite ablation products and their contribution to the atmospheres of terrestrial planets: An experimental study using pyrolysis-ftir. *Geochimica et Cosmochimica Acta* **73**, 3512–3521 (2009).
 44. G Tobie, D Gautier, F Hersant, Titan's bulk composition constrained by cassini-huygens: Implication for internal outgassing. *The Astrophys. J.* **752**, 125 (2012).
 45. G Tobie, JI Lunine, C Sotin, Episodic outgassing as the origin of atmospheric methane on titan. *Nature* **440**, 61–64 (2006).
 46. A Levi, D Sasselov, M Podolak, Structure and dynamics of cold water super-earths: The case of occluded ch₄ and its outgassing. *The Astrophys. J.* **792**, 125 (2014).
 47. TL Schindler, JF Kasting, Synthetic spectra of simulated terrestrial atmospheres containing possible biomarker gases. *Icarus* **145**, 262–271 (2000).
 48. C Oze, LC Jones, JI Goldsmith, RJ Rosenbauer, Differentiating biotic from abiogenic methane genesis in hydrothermally active planetary surfaces. *Proc. Natl. Acad. Sci.* **109**, 9750–9754 (2012).
 49. A Neubeck, NT Duc, D Bastviken, P Crill, NG Holm, Formation of h₂ and ch₄ by weathering of olivine at temperatures between 30 and 70 c. *Geochem. Transactions* **12**, 10 (2011).